Identification and Characterization of Dual Inhibitors of the USP25/ 28 Deubiquitinating Enzyme Subfamily

Wrigley, J. D., Gavory, G., Simpson, I., Preston, M., Plant, H., Bradley, J., Goeppert, A. U., Rozycka, E., Davies, G., Walsh, J., Valentine, A., McClelland, K., Odrzywol, K. E., Renshaw, J., Boros, J., Tart, J., Leach, L., Nowak, T., Ward, R. A., ... Andrews, D. M. (2017). Identification and Characterization of Dual Inhibitors of the USP25/ 28 Deubiquitinating Enzyme Subfamily. *ACS Chemical Biology*. https://doi.org/10.1021/acschembio.7b00334

Document Version:
Peer reviewed version

Queen's University Belfast - Research Portal:
Link to publication record in Queen's University Belfast Research Portal

Title:

Identification and characterisation of dual inhibitors of the USP25/28 Deubiquitinating enzyme subfamily.

Authors:

Jonathan D. Wrigley[a]*[#], Gerald Gavory[c#], Iain Simpson[b], Marian Preston[a], Helen Plant[a], Jenna Bradley[a], Anne U. Goeppert[a], Ewelina Rozycka[c], Gareth Davies[a], Jarrod Walsh[a], Andrea Valentine[c], Keeva McClelland[c], Krzysztofa Ewa Odrzywol[c], Jonathan Renshaw[a], Joanna Boros[a], Jonathan Tart[a], Lindsey Leach[a], Thorsten Nowak[b], Richard A. Ward[b], Timothy Harrison[c] & David M Andrews[b]

#Joint Co-authors

Address:

[a]Discovery Sciences, IMED Biotech Unit, AstraZeneca, Cambridge, United Kingdom

[b]Oncology, IMED Biotech Unit, AstraZeneca, Cambridge, United Kingdom

[c]Almac Discovery Ltd, Centre for Precision Therapeutics, 97 Lisburn Road, BT9 7AE, United Kingdom.

*Corresponding Author

Dr. Jonathan Wrigley

IMED Biotech Unit, AstraZeneca, Unit 310 - Darwin Building, Cambridge Science Park, Milton Rd, Cambridge CB4 0FZ

Tel: (+44) 01625 235830

Fax: (+44) 01625 519749

Email: jonathan.wrigley@astrazeneca.com

Word Count: 8002

(Abstract, Body Text, Methods, References, Figure legends)

 ABSTRACT

The Ubiquitin Proteasome System is widely postulated to be a new and important field of drug discovery for the future, with the Ubiquitin Specific Proteases (USP) representing one of the more attractive target classes within the area. Many USPs have been linked to critical axes for therapeutic intervention, and the finding that USP28 is required for c-Myc stability suggests that USP28 inhibition may represent a novel approach to target this so far undruggable oncogene. Here we describe the discovery of the first reported inhibitors of USP28, which we demonstrate are able to bind to and inhibit USP28, and whilst displaying a dual activity against the closest homologue USP25, these inhibitors show a high degree of selectivity over other deubiquitinases (DUBs). The utility of these compounds as valuable probes to investigate and further explore cellular DUB biology is highlighted by the demonstration of target engagement against both USP25 and USP28 in cells. Furthermore, we demonstrate that these inhibitors are able to elicit modulation of both the total levels and the half-life of the c-Myc oncoprotein in cells, and also induce apoptosis and loss of cell viability in a range of cancer cell lines. We however observed a narrow therapeutic index compared to a panel of tissue-matched normal. Thus, it is hoped that these probes and data presented herein will further advance our understanding of the biology and tractability of DUBs as potential future therapeutic targets.

GRAPHICAL TABLE OF CONTENTS ENTRY
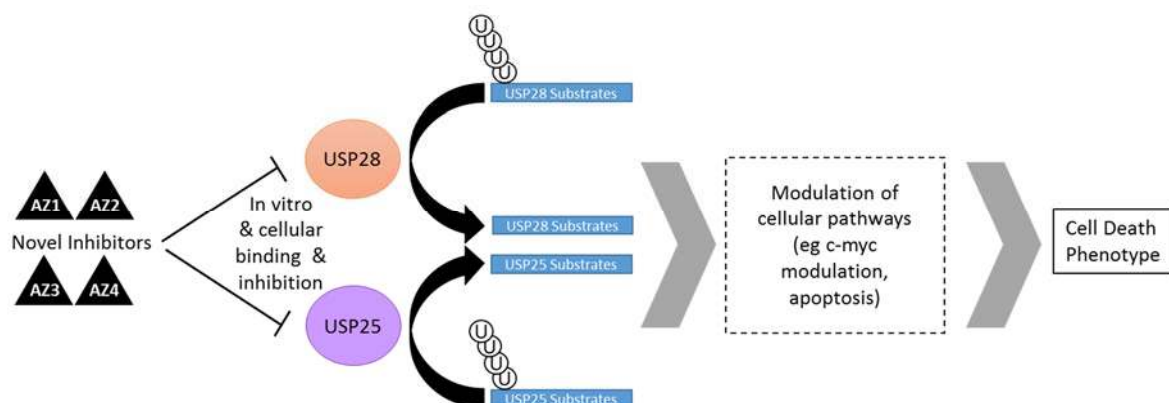
INTRODUCTION

Whilst considerable progress has been made in enabling the efficient discovery and development of therapeutic agents for a wide range of disease areas, many challenges still remain, including the high attrition rates of molecules in development and a reliance on historically tractable target classes, such as kinases[1]. For these reasons, significant effort has been devoted towards identifying and generating hit molecules directed against new target classes that may represent novel axes for therapeutic intervention. The growing disease linkage and essentiality to many cellular processes, make the Ubiquitin Proteasome System (UPS) an attractive target class for the discovery of new therapeutic entities[2, 3].

The UPS represents the major eukaryotic pathway for selective proteolysis of intracellular proteins, through the concerted action of E1, E2 & E3 ubiquitin ligases which elicit protein regulation by the addition of the 76 amino-acid Ubiquitin (Ub) molecule in chains of varying length and linkage complexity [4]. Notably, the ability to generate and attach a wide variety of different Ub chains to proteins through attachment at specific amino acid residues via different linkages, equips the cell with a highly sophisticated means of directing proteins towards a variety of cellular outcomes. One such example is the attachment of four or more Lysine 48-linked Ubiquitin moieties to a protein which generally targets it for proteasomal degradation. The ubiquitination process is reversible and an additional layer of regulation is afforded to the cell through the action of deubiquitinating enzymes (DUBs), which cleave Ub from the target and are thereby able to reverse the process, precluding for instance proteasomal destruction.

DUBs comprise a large family of mostly cysteine proteases, split into sub-families of which the Ubiquitin Specific Protease family (USPs) is the largest[5]. Through cleavage of the isopeptide bond between the C-terminal Gly76 of Ub and the ε-amino group of the lysine residue of the target protein, the enzymes modulate a wide range of cellular axes, with growing linkages to cancer-associated pathways[6-8]. It is therefore anticipated that, building on the success of the proteasome inhibitor Bortezimib (Velcade) in multiple myeloma[9], both the DUBs in general[2] and USPs in particular may represent a rich source of novel therapeutic agents.

Despite a growing number of linkages between DUBs and key disease loci, drug discovery in this area remains in its infancy, and to date has been focussed on a small number of enzymes[10-12]. Furthermore, whilst the recent identification of several inhibitors of USP1[13], USP7[14, 15], USP8[16], USP9x[17] and USP14[18] yields promise, the general challenges in identifying leads with a clear mechanism of action, phenotypic effect and profile suitable for progression towards a clinical candidate remain to be overcome[19, 20]. Thus, a crucial step in the development of this potential target class is the identification and characterisation of hit molecules against novel DUBs, to further increase our knowledge of both chemical tractability and biological potential for modulation of key cellular pathways.

One such potential opportunity arose following the discovery by Popov and colleagues in 2007 that USP28 is able to bind to and preclude proteasomal degradation of c-Myc through an interaction with the Fbw7α ubiquitin E3 ligase[21]. Although the c-Myc proto-oncogene was discovered over 30 years ago, from a drug discovery perspective it remains a challenging, yet attractive target[22, 23]. Further relevance of USP28 as a potential therapeutic target comes from the growing association between expression of USP28 and Fbw7 and a range of tumour types[24-27]. However, c-Myc regulation is highly complex[28], and furthermore additional reports have suggested that the USP28 / c-Myc relationship is not straight forward, with an apparent dual regulation, resulting in either elevation or downregulation of Fbw7 substrates depending on the degree of USP28 loss[29]. Whilst further characterisation of c-Myc regulation is thus needed, the prospect of indirectly targeting and modulating c-Myc levels by targeting USP28 prompted us to initiate a screening campaign for the *de novo* identification of hits against this target of potentially high clinical relevance.

Here we describe the use of a high throughput screening (HTS) approach to successfully identify the first reported USP28 inhibitors, which have been characterised in a range of biochemical and cellular assays. We demonstrate not only that these compounds inhibit USP28 *in vitro*, but also confirm by two independent methods, that they directly and productively bind to USP28. We also show that whilst these inhibitors possess a high degree of *in vitro* selectivity over most DUB family

members they possess equipotent activity against the closest related homologue, USP25. Initial cellular characterisation supported the *in vitro* data demonstrating that the compounds engage both USP28 and USP25. These inhibitors were then used as chemical probes to start investigating the biology of USP28. These studies demonstrated direct modulation of USP28 substrates in cells, including total c-Myc levels in cells. This effect was achieved through modulation of the half-life of c-Myc via a proteasome-dependent mechanism. Further cellular characterisation shows that these inhibitors cause induction of apoptosis and affect cell viability across a range of cancer cell lines but with a minimal window compared to a panel of normal cell lines. Together these data highlight the utility of these probe molecules in the further characterisation of both this cellular pathway and wider DUB biology, which will be required for the generation of novel therapeutics against this target class.

RESULTS & DISCUSSION

As outlined above, the identification of USP28 inhibitors would add considerable value to the growing Ubiquitin drug discovery field, through both enabling better characterisation of the cellular DUB activity and also providing start points for the development of therapeutic molecules. In order to achieve this, we employed a high throughput screening strategy using purified recombinant USP28 enzyme and a fluorogenic substrate consisting of Ubiquitin derivatised at the C-terminus with Rhodamine-110 (Ub-Rh110)[30] . A comprehensive assay development was performed, as described in the supporting information, including analysis and optimisation of the assay time course, Km determination, effect of reducing agents, Z′ analysis[31] and validation with a broad-spectrum inhibitor (Supporting information, Figure S1a-d). Following completion of the assay development and validation phases, a high throughput screening (HTS) campaign was run using a directed library of approximately 40,000 compounds. Around half of these compounds were selected as a representative set of the AstraZeneca full compound collection, favouring scaffolds with a range of near-neighbours for follow-up testing. The other half consisted of compounds which have shown activity against one or more protease assays within AstraZeneca.

The HTS campaign yielded a primary hit rate of approximately 5.3%, and primary hits were subsequently analysed in a "ratio-test" assay[32] format to assess specificity (Figure S1e-f). A "ratio test" was performed to assess specificity of the hits, by screening the compounds on two occasions. The first occasion utilised the assay conditions determined for primary screening whilst the second employed 10-fold higher levels of enzyme, but tested over a 10-fold shorter timescale. For compounds that specifically inhibit the enzyme (i.e. non-spurious, non-promiscuous), the inhibition profile and IC_{50} value should be identical under both conditions. However, compounds that inhibit via a non-specific mechanism (e.g. aggregator or reactive compounds), are expected to display a shift in the IC_{50} values between the two conditions. The data clearly showed both a population of likely "specific" inhibitors (whose profiles do not alter, n= 15), and a second population of 10-fold shifted (and therefore likely non-specific, false positive) hits (n=27) (supplementary information Figure S1f).

By combining data from the "ratio-test" assay with chemo-informatic analysis (solubility, redox activity) of the USP28 primary screening data we selected a subset of 42 compounds for further profiling.

As part of the validation phase by titration, a series of benzylaminoethanols represented by AZ1, AZ2 and AZ4, were identified which exhibited IC_{50} values of 0.7, 1.1 and 2.0 µM respectively (Table 1). Interestingly, our studies also revealed a structurally related but significantly less active inhibitor namely AZ3 with an IC_{50} value of 59.6 µM (Table 1). Since identification of these compounds, more physiologically relevant substrates have been brought into use, such as Di-Ubiquitin[33], the isopeptide linked Ubiquitin-tetramethyrhodamine (Ub-TMR) substrate and the tetra-ubiquitin chain Tetra-Ub. For comparative purposes, additional studies were subsequently performed with the latter two of these substrates and the compounds exhibited similar IC_{50} values with these more physiologically relevant substrates (Table 1). Further characterisation of this class of compounds was then performed, commencing with binding validation using orthogonal biophysical techniques.

For these binding studies, two independent biophysical techniques were utilised, the first of which was Isothermal Titration Calorimetry (ITC). This label free methodology directly measures the heat of binding for the interaction that occurs when a ligand binds to a target protein, and can be used to confirm ligand binding, calculate the equilibrium dissociation constant (K_d), and stoichiometry of the interaction. These parameters are additionally useful to characterize the binding interaction and to demonstrate the functional integrity of the enzyme. Under the conditions of our experiments, K_d values of 0.2, 0.9 & 2.7 µM were derived for AZ1, AZ2 & AZ4 respectively (Figure 1a-c; Table 1), whilst the less active close analogue AZ3 failed to produce a measurable K_d value. These values are consistent with the biochemical activity data described previously. In addition, corresponding stoichiometry values of 0.6, 0.7 & 0.8 were derived for AZ1, AZ2 & AZ4 respectively (Fig. 1a-c) in line with a non-spurious and specific mode of binding, hence supporting our initial observations from the "ratio test" experiments. For comparison, two compounds determined by the "ratio test" as potentially acting via alternative mechanisms were also tested and produced noisy and difficult to interpret data (data not shown). The second approach taken to confirm binding of the

compounds to USP28 utilised the NanoTemper Microscale Thermophoresis (MST) methodology, which produced comparable data. In this instance, K_d values of 3.7, and 10.3 μM were determined for AZ1 and AZ2 respectively (Supporting information Figure S2a-b and Table 1). In agreement with the ITC data AZ3 failed to produce a determinable result. The binding constants for the compounds were determined using the protein's intrinsic fluorescence. We believe this resulted in a less sensitive detection system than the fluorescently labeled version of the approach. This may in part account for the apparent discrepancy in K_d estimates between MST and ITC. In contrast AZ4 generated a K_d using the labeled protein which was in much closer agreement with the ITC result (3.6 *vs* 2.7 μM; Table 1). Despite K_d values being higher than the IC_{50} values obtained in the *in vitro* enzyme assay and the K_d values from our ITC experiments further confirm target-ligand engagement. Taken together these data derived from two independent methodologies demonstrate AZ1, AZ2 and AZ4 interact with and bind to USP28 in a non-spurious and specific manner.

Building upon these studies and performing a high-dilution assay format, we also demonstrated that these inhibitors bind reversibly to the USP28 target. Briefly, in this assay USP28 was pre-incubated with 10 times the IC_{50} concentration of the inhibitor (where full inhibition is expected), followed by 100-fold dilution. USP28 activity is then re-assessed and full restoration of the activity is expected upon re-equilibration in the case of a reversible binder as observed with the inhibitors AZ1-AZ4 (Supplementary information; Figure S5). This data is also consistent with the lack of any reactive functionality on these molecules. Iodoacetamide was used in these experiments as a non-specific alkylator and irreversible inhibitor of DUBs.

Following the reversibility studies, kinetic experiments were subsequently performed to characterise the mode of inhibition of USP28 using the most potent compound AZ1 as a representative example. In these studies, we assayed USP28 across a range of Tetra-Ub substrate concentrations in the presence of increasing concentrations of inhibitor. Lineweaver-Burk analysis revealed that AZ1 acts as a non-competitive inhibitor (Supporting information Figure S6). The apparent K_m value for Tetra-Ub was calculated as 8.6 μM and the inhibitory constant for AZ1 derived from this analysis (K_i = 1.5 μM) was in excellent agreement with the IC_{50} value obtained previously (IC_{50} = 0.7–1.0 μM; Table 1).

With clear and robust inhibitory activity demonstrated against USP28, we next assessed the selectivity profiles of AZ1–AZ4 against representative USPs and DUBs. To this end, and as part of our internal validation process, AZ1–4 were routinely counter-screened against the USP2a protein. All compounds were found to be inactive against this particular DUB with IC_{50} values >100 µM (Table 1). AZ1–3 were subsequently profiled against an extended and commercially available panel of DUBs (Ubiquigent), which included 14 USPs (USPs1, 2, 4, 5, 7, 11, 15, 19, 20, 25, 28, 36, 45 & CYLD), and 8 further DUBs comprising 4 UCHs (UCHL1, UCHL3, UCHL5 & BAP1), 3 OTUs (OTUB2, OTUD6B, Cezanne) and 1 JAMM (AMSH-LP). The data obtained in these Ub-Rho110-based assays (performed at 10 µM fixed inhibitor concentration) demonstrated strong inhibition of both USP28 & USP25 (>90%), whilst no significant effect was observed against any of the other family members tested (<10% inhibition; Fig. 2a). Our most potent inhibitor AZ1 was subsequently taken as a representative example and tested at a fixed concentration of 30 µM (i.e. >40-fold IC_{50} USP28) against representative caspases and cathepsins. Under the conditions of these experiments, no off-target effects were observed against any of these cysteine proteases (<25% inhibition; Supporting information, Figure S7). Thus, under the conditions of these experiments, the compounds appear to be potent inhibitors of USP28 & USP25 and highly selective over all other 20 DUBs included in this panel and over a selection of other non-related proteases. To the best of our knowledge these compounds represent the first validated inhibitors of either USP28 or USP25.

Based on these data, we further characterised the ability of the compounds to inhibit USP25 *in vitro* with follow-up titration studies for IC_{50} determination. Parallel dose-response testing of AZ1, 2, & 3 in purified enzyme assays demonstrated that all three compounds appear approximately equipotent against USP28 and USP25 (Fig 2b-e). In concordance with our previous studies, AZ3 was found to be only weakly active against USP25 with 30% inhibition at 10 µM and an IC_{50} value of 26.4 µM. This dual activity can be explained by the high degree of homology (>50% nucleotide and amino acid identity & highly conserved exon-intron boundaries) between USP28 and its structurally closest analogue, USP25[34], and is indicative that, whilst identification of compounds with broad selectivity across the DUB family is achievable, obtaining

selectivity between the closest homologues may represent, in some circumstances, a significant challenge.

Following the extensive *in vitro* profiling described above, we next wanted to determine whether these inhibitors were able to directly engage USP28 in a cellular environment. To this aim, activity-based profiling studies were carried out using the Ubiquitin-vinyl sulfone substrate (Ub-VS) as molecular probe. Ub-VS is a potent and reactive inhibitor of DUBs and its covalent interaction with the enzyme can be detected by mobility shift in western blotting analysis. As shown in Figure 3a, increasing concentration of the inhibitors AZ1, AZ2 and AZ4 initially reduced and ultimately ablated, in a concentration dependant manner, the covalent labelling of USP28 by Ub-VS. Densitometry analyses were subsequently performed and EC_{50} values of 5.3, 18.2 and 11.3 μM were derived from these experiments for AZ1, AZ2 and AZ4 respectively. In contrast, AZ3 had no significant effect at either 60 or 100 μM (Fig. 3a). These data corroborate our previous biochemical and biophysical studies and unambiguously demonstrate direct evidence for target occupancy in cells.

In response to the observation of activity against USP25 in an *in vitro* enzyme assay, we next performed additional cellular target engagement assays to determine whether the inhibitors interacted with USP25 in a cellular context. These data clearly demonstrate that in parallel to interacting with USP28, AZ1, AZ2 & AZ4 are also able to engage with USP25 with EC_{50} values of 3.3, 11.5 and 19.6 μM respectively (Fig 3b.). In contrast, target engagement of less-closely related DUB family members such as USP7 and USP4 was not observed up to 60 μM, in line with the DUB screening panel data (Fig 3c.). The potency and selectivity profiles of AZ1, AZ2 and AZ4 combined with good physicochemical properties (Molecular Weight <500, $LogD_{7.4}$ in the 2.7-3.5 range and good solubility (Table 1)), made them suitable molecular and functional probes for further cellular investigations.

Since the primary goal of our screening campaign was the identification of USP28 inhibitors, we next prioritised proof-of-concept cellular studies using these validated inhibitors, to probe the regulation of endogenous c-Myc protein levels by USP28 in the HCT116 colon carcinoma cell line. HCT116 was used as a model cell line for our initial mechanistic studies based on both the high USP28 expression and also

precedence from the Popov *et al.* studies[21] demonstrating regulation of c-Myc protein levels by USP28 using siRNA. Cells were treated with increasing concentrations of compounds and samples were collected after 3 hrs for analysis. As shown in Figure 4a, western blotting analyses indicate a rapid and concentration-dependant decrease in c-Myc total protein levels following treatment with AZ1 and AZ2. Complete reduction in c-Myc levels was observed in both cases at the highest concentrations tested. Importantly, the decrease in c-Myc levels could not be attributed to total protein degradation following compound treatment as evidenced by the steady state levels in the loading control β-actin or USP28. Similar studies performed with the less active structurally related compound AZ3 only showed an effect on c-Myc levels at the highest concentration of 100 μM (and to a much lesser extent at 80 μM). No significant effect was detectable at 60 μM or below (Fig. 4a). Together, the relative activity of the three compounds correlates well with their activity in the biochemical and target engagement assays described previously.

Furthermore, AZ1 and AZ2 were observed to induce apoptosis in a rapid and concentration-dependant manner as evidenced by the cleavage of full-length PARP into a smaller (85 kDa) adduct (Fig. 4a). Interestingly, the concentration-dependent reduction in c-Myc levels was mirrored by a concomitant increase in PARP cleavage. Apoptosis induction was most pronounced following complete down-regulation of c-Myc. Under the conditions of these experiments, no PARP cleavage or apoptosis was detected following treatment with AZ3 up to 100 μM (Fig. 4a). Subsequently, we decided to extend our investigations beyond HCT116 cells and demonstrated that similar trends and effects were observed in multiple other cell lines including the colorectal adenocarcinoma SW480 and HT29 lines (Fig. S3a-b).

Next, a series of experiments were performed in an attempt to elucidate the mechanism responsible for the rapid decrease in c-Myc total protein levels following compound treatment. To determine whether the decrease in total c-Myc protein levels was mediated through the proteasome, HCT116 cells were pre-treated with both cycloheximide (CHX) and the proteasome inhibitor MG-132, followed by treatment with compound AZ1 or vehicle as a control. Samples were subsequently collected at various timepoints for western blot analysis probing for c-Myc levels. As shown in Fig. 4b, MG132 efficiently blocked the reduction in total c-Myc abundance resulting

in steady state levels of the protein for up to 180 min (the longest timepoint investigated). Under the conditions of these experiments and following densitometry analysis, the half-life of c-Myc was determined to be 72 min in untreated cells whilst treatment with AZ1 significantly reduced this value by almost 50% to 40 min. Together, these studies demonstrate that the observed reduction in total c-Myc protein levels is mediated by proteasomal degradation.

Flow cytometry analysis was then performed to assess the effect of the compounds over a longer time-period. The study demonstrated cell death induction in a dose-dependent manner, as evidenced by the accumulation of a sub-G1 population (Supporting information; Figure S4). Based on these data, the anti-proliferative effect of these compounds was subsequently investigated. Briefly, cells were treated with increasing concentrations of the compounds (up to 100 µM) and cell viability was assessed after 72 hrs. In good agreement with the observed sub-G1 population accumulation, our data demonstrate a dose-dependent loss of cell viability with EC_{50} values of 18.0-20.0 µM range for AZ1 and AZ2 (Fig. 5a). Under the same conditions, AZ3 was approximately 3-fold less active exhibiting an EC_{50} value of 93.2 µM. Similar effects on viability were observed in the HT29 and SW480 cell lines (Fig. 5a; EC_{50} values compiled in Supplementary Table 1). Altogether, these studies demonstrated that AZ1 and AZ2 inhibitors are able to induce both dose and time dependent cell cycle perturbations and cell death resulting in an anti-proliferative response.

In order to further characterise the potential therapeutic opportunity afforded by these compounds, their effect on cell viability was monitored across a broader range of tumour cell lines from different tissue of origins and also tissue-matched normal cells. In total, a representative panel of 29 cell lines was used in this study including 22 cancer cell lines and 7 tissue-matched normal cell lines. Proliferation assays were performed as described previously and the compiled dataset is shown in Fig. 5b & compiled in Supplementary Table 1. Our data demonstrated that AZ1 and AZ2 were able to reduce cell viability across a range of cancer cell lines with EC_{50} values typically clustered around 20 µM. Further analysis however indicated that no significant differentiation in response was observed between tumour and normal cell types (Fig. 5b). A minimal window of 3-5-fold was still typically observed between

the active compounds AZ1 and AZ2, and the less active analogue AZ3, in both the normal and cancer sets. We attempted to further optimise and develop these initial studies to improve this narrow therapeutic index. To this end, longer term viability assay (up to 7 days) and clonogenic assays (up to 12 days) were carried out but with little effect on the cancer to normal cell lines window. Similarly, changing the treatment modality in these assay formats to repeated or pulse treatments brought no further improvement (data not shown). We believe that this lack of selective killing results from the complexity of the pathways involved and potential redundancy between family members, such that the oncogenic effects of any specific gene amplifications, for example, are minimised. This hypothesis of a more complex scenario could be further investigated through the generation of a panel of genome-edited cell lines (e.g. CRISPR/Cas9-based), to characterise both the compounds and pathways in knockout models. Furthermore, it is hoped that further optimisation of these compounds may improve both potency and selectivity, which is likely to improve the therapeutic index.

The studies described herein report the identification and early characterisation of the first reported inhibitors of USP28 and USP25, which are able to bind to and inhibit both recombinant and endogenous enzymes. These inhibitors exhibit good biochemical potency and binding affinity as well as excellent selectivity profiles against a broader panel of DUBs. In cells, these compounds engage both targets and induce a dose-dependent reduction in the endogenous levels of a reported USP28 substrate c-Myc, which we showed is mediated by the proteasome. Further cellular profiling demonstrated that these compounds induce apoptosis and in turn exert an anti-proliferative effect in both cancer and normal cell lines, albeit with no significant window in response. Whilst the observed c-Myc modulation is consistent with previous reports of the action of USP28[21], we cannot exclude the possibility that the apoptotic and cell viability phenotypic effects are arising as a result of parallel inhibition of both USP25 and USP28. For example, it is plausible that whilst c-Myc-driven effects may result from USP28 inhibition, other phenotypic observations, such as the induction of PARP cleavage could result from an alternative action on USP25. Therefore, the potential for redundancy to occur within the DUB family, coupled with the challenge of obtaining selectivity between closely related family members (e.g. as

previously reported between USP7 and USP47[35]), represent key challenges to be considered in the generation of therapeutic inhibitors of USPs.

Given the limited number of quality, reversible inhibitors published to date, it is anticipated that these detailed studies and orthogonally validated probes will be of significant utility to the broad research community. Firstly, since these molecules represent the first reported inhibitors of both enzymes, they should enable further investigation of the cellular biology related to USP25 and USP28, as well as probing the selectivity and redundancy between these closely related DUBs. For example, proteomic analysis following treatment of cells with these inhibitors may help characterisation of both their action and in turn reveal the complexity and interplay of DUB activities.

Further development and optimisation of these scaffolds to improve both potency, and selectivity between USP25 and USP28, may not only aid such investigations, but may potentially improve the therapeutic index between activity in normal and cancer cells. Additionally, these probe compounds could act as seeds and provide templates for the development of inhibitors of USP28, USP25 and other members of this challenging target class. Indeed, our demonstration of the ability to identify broadly selective small molecules able to both bind to and inhibit USP targets *in vitro* and in cells, and the fact that the issues of selectivity and redundancy are likely to be target specific, provides encouragement that therapeutically relevant USP inhibitors can be developed in the future.

MATERIALS & METHODS

Chemistry:

Compounds AZ1-4 were prepared as described in the Supporting Information.

Binding Assays – Isothermal Titration Calorimetry

The USP28 protein and test compounds were dialysed in 40 mM HEPES (pH 7.5), 150 mM NaCl, in order to minimise heat effects due to buffer mismatch or ionisation.   ITC experiments were carried out with 20 µM USP28 protein, contained in the cell of a Microcal iTC200 instrument, titrated with 200 µM test compound, contained in the instrument injection syringe. The interaction of USP28 with test compound was quantified using a Microcal ITC 200 (GE healthcare). The titration data were recorded at 25 °C in 40 mM HEPES pH 7.5, 150 mM NaCl, 2% DMSO. Aliquots of 200 µM ligand stocks were added to 20 µM USP28 in multiple 2 µL intervals. Data was analysed using non-linear least squares regression using Microcal Origin software (GE healthcare).

USP Selectivity Assessment

The selectivity of compounds across the DUB family was analysed through testing in the DUBProfiler panel at Ubiquigent (www.ubiquigent.com). This involved inclusion of test compounds at a concentration of 10 µM in a range of Ub-Rho110 *in vitro* enzyme assays. Enzyme assays were generated and run for the following DUB-family members: 14 USPs (USPs1, 2, 4, 5, 7, 11, 15, 19, 20, 25, 28, 36, 45 & CYLD), 4 UCHs (UCHL1, UCHL3, UCHL5 & BAP1), 3 OTUs (OTUB2, OTUD6B, Cezanne) and 1 JAMM (AMSH-LP). Data generated is displayed as a percentage inhibition of total enzyme activity for each enzyme. Dose response testing against USP28 and USP25 was performed in the same way, testing compounds in the range of 100-0.03µM. Selectivity of AZ1 against cysteine proteases including caspases 1/2/4/5/8 and cathepsins H/L/S was tested at a fixed screening concentration of 30 µM and data reported as % of enzyme activity relative to DMSO control (Reaction Biology).

Cell Assays

In order to assess cellular activity of the compounds, HCT116 cells were treated with USP28 inhibitor compounds for a period of 3 hrs. Following this incubation, cells were harvested, lysed and subjected to Western Blot analysis. Samples were probed for c-Myc protein levels and also probed for β-actin levels, as a loading control. In

order to determine the half-life of c-Myc in cells, HCT116 cells were treated for 3 hr with USP28 inhibitors in the presence of cycloheximide (100 μg/ml) to block nascent protein synthesis. Thus any alteration in c-Myc levels would be indicative of changes in degradation as opposed to protein synthesis. Following compound treatment, cells were harvested and lysed prior to Western blot analysis

Cells lines and culture conditions

All cell lines were obtained from the American Type Culture Collection (ATCC), and were both authenticated by STR profiling (Promega) and shown to be mycoplasma-free through external (Cell Check 9 Plus; IDEXX BioResearch) or internal testing with the MycoAlert mycoplasma detection (Lonza; LT07-318). For growth, cells were maintained at 37°C in a humidified atmosphere with 5% CO_2. HCT116 and HT29 were cultured in McCoys 5A supplemented with 10% (v/v) FBS, 1% (v/v) Penicillin/streptoMycin, 1% (v/v) L-Glutamine. DU145, LNCAP, PC3, PNT2, A549 and OVCAR8 were cultured in RPMI supplemented with 10% (v/v) FBS, 1% (v/v) Penicillin/streptoMycin, 1% (v/v) L-Glutamine. InMyo Fib were cultured in Smooth Muscle Cell Basal Medium (Lonza). NL20 were cultured in F-12, Ham Nutrient Mixture supplemented with 4% (v/v) FBS, 1% (v/v) Penicillin/streptoMycin, 1% (v/v) L-Glutamine, 1% (v/v) NEAA, 5μg/ml of Insulin (Sigma Aldrich), 0.05 μg/ml of transferrin, 0.5 μg/ml of hydrocortisone (Sigma Aldrich) and 0.05 μg/ml of EGF (Sigma Aldrich). U87MG, U251 and A431 were cultured in DMEM supplemented with 10% (v/v) FBS, 1% (v/v) Penicillin/ streptoMycin, 1% (v/v) L-Glutamine. HMEC-1 were cultured in MCDB-131 supplemented with 10% (v/v) FBS, 1% (v/v) Penicillin/streptoMycin, 1% (v/v) L-Glutamine, EGF 1 ng/ml. Medium and supplements were purchased from Life Technologies except were indicated.

Reagents for cellular characterisation

The USP28 inhibitors (AZ1, AZ2, AZ3 and AZ4) were prepared as 100 mM DMSO stocks for cell culture experiments. Cycloheximide was purchased from Calbiochem and used at a final concentration of 100 μg/mL. MG132 and Propidium Iodide (PI) were both obtained from Sigma-Aldrich and used at a final concentration of 20 μM and 10 μg/mL respectively. RNaseA was purchased from Qiagen and used at a final concentration of 250 μg/mL. CellTitre-Glo (cell viability assay) was purchased from

Promega. Ubiquitin-Vinyl Sulfone (Ub-VS) was purchased from Boston Biochem and used at a final concentration of 32 µg/ml.

Western blotting and antibody sources

Cells were lysed in radioimmuno-precipitation (RIPA) buffer containing 50 mM Tris HCl (pH 7.6), 150 mM NaCl, 1 mM EDTA, 1% NP40, 0.25% Na-deoxycholate and supplemented with a phosphatase (PhosSTOP, Roche) and protease inhibitor cocktail tablet (cOmplete Mini, Roche). Antibodies were obtained from AbCam; anti-USP28 (Ab110744; 1:1000 dilution), anti-USP25 (ab187156; 1:1000), BD Bioscience;; anti-USP28 (A300-898A; 1:1000), Cell Signaling; anti-c-Myc (5605; 1:1000) and anti-PARP (9542; 1:1000), anti-USP28 (4217, 1:1000), Santa Cruz; anti-β-actin (A5316; 1:5000), HRP conjugated anti-rabbit (A0545 1:5000) and HRP conjugated anti-mouse (A9917; 1:5000).

Target engagement assay

HCT116 cells were treated with USP28 inhibitors for 2 hr. Following incubation, cells were harvested in TE lysis buffer containing 50 mM Tris (pH7.4), 150 mM NaCl, 5 mM MgCl2, 0.5 mM EDTA, 0.5% NP40, 10% Glycerol, 2 mM DTT and clarified cell lysates (40 µg) incubated with Ubiquitin-vinyl Sulfone in assay buffer containing 50 mM Tris (pH7.6), 5 mM $MgCl_2$, 250 mM Sucrose, 0.5 mM EDTA, 2 mM DTT for 1 hr on ice. The reaction was terminated by the addition of LDS sample buffer (Life Technologies) and heated to 70ºC. Samples were then analysed by western blotting.

Proliferation Assays

Cells were typically seeded in 96 well plate format (typically 4000-6000 cells/well) and treated after 24 hrs with increasing concentration of compound from 0 to 100 µM in ½ log unit increments. Cell viability was assessed after 72 hrs by CellTiter-Glo® as recommended by the manufacturer's instructions (Promega). Analysis and EC_{50} values were derived using GraphPadPrism.

ACKNOWLEDGEMENTS

Supporting Information Available:
This material is available free of charge *via* the Internet.

REFERENCES

[1] Paul, S. M., Mytelka, D. S., Dunwiddie, C. T., Persinger, C. C., Munos, B. H., Lindborg, S. R., and Schacht, A. L. (2010) How to improve R&D productivity: the pharmaceutical industry's grand challenge, *Nat Rev Drug Discov 9*, 203-214.

[2] Cohen, P., and Tcherpakov, M. (2010) Will the ubiquitin system furnish as many drug targets as protein kinases?, *Cell 143*, 686-693.

[3] Nalepa, G., Rolfe, M., and Harper, J. W. (2006) Drug discovery in the ubiquitin-proteasome system, *Nat Rev Drug Discov 5*, 596-613.

[4] Komander, D. (2009) The emerging complexity of protein ubiquitination, *Biochem Soc Trans 37*, 937-953.

[5] Nijman, S. M., Luna-Vargas, M. P., Velds, A., Brummelkamp, T. R., Dirac, A. M., Sixma, T. K., and Bernards, R. (2005) A genomic and functional inventory of deubiquitinating enzymes, *Cell 123*, 773-786.

[6] Komander, D., Clague, M. J., and Urbe, S. (2009) Breaking the chains: structure and function of the deubiquitinases, *Nat Rev Mol Cell Biol 10*, 550-563.

[7] Reyes-Turcu, F. E., Ventii, K. H., and Wilkinson, K. D. (2009) Regulation and cellular roles of ubiquitin-specific deubiquitinating enzymes, *Annu Rev Biochem 78*, 363-397.

[8] Sacco, J. J., Coulson, J. M., Clague, M. J., and Urbe, S. (2010) Emerging roles of deubiquitinases in cancer-associated pathways, *IUBMB Life 62*, 140-157.

[9] Adams, J., and M., K. (2004) Development of the Proteasome Inhibitor Velcade TM (Bortezomib), *Cancer Investigation 22*, 304-311.

[10] Nicholson, B., Marblestone, J. G., Butt, T. R., and Mattern, M. R. (2007) Deubiquitinating enzymes as novel anticancer targets, *Future Oncology 3*, 191-197.

[11] Daviet, L., and Colland, F. (2008) Targeting ubiquitin specific proteases for drug discovery, *Biochimie 90*, 270-283.

[12] Harrigan, J. A., Jacq, X., Martin, N. M., and Jackson, S. P. (2017) Deubiquitylating enzymes and drug discovery: emerging opportunities, *Nat Rev Drug Discov*.

[13] Liang, Q., Dexheimer, T. S., Zhang, P., Rosenthal, A. S., Villamil, M. A., You, C., Zhang, Q., Chen, J., Ott, C. A., Sun, H., Luci, D. K., Yuan, B., Simeonov, A., Jadhav, A., Xiao, H., Wang, Y., Maloney, D. J., and Zhuang, Z. (2014) A selective USP1-UAF1 inhibitor links deubiquitination to DNA damage responses, *Nat Chem Biol 10*, 298-304.

[14] Colland, F., Formstecher, E., Jacq, X., Reverdy, C., Planquette, C., Conrath, S., Trouplin, V., Bianchi, J., Aushev, V. N., Camonis, J., Calabrese, A., Borg-Capra, C., Sippl, W., Collura, V., Boissy, G., Rain, J. C., Guedat, P., Delansorne, R., and Daviet, L. (2009) Small-molecule inhibitor of USP7/HAUSP ubiquitin protease stabilizes and activates p53 in cells, *Mol Cancer Ther 8*, 2286-2295.

[15] Reverdy, C., Conrath, S., Lopez, R., Planquette, C., Atmanene, C., Collura, V., Harpon, J., Battaglia, V., Vivat, V., Sippl, W., and Colland, F. (2012) Discovery of specific inhibitors of human USP7/HAUSP deubiquitinating enzyme, *Chem Biol 19*, 467-477.

[16] Colombo, M., Vallese, S., Peretto, I., Jacq, X., Rain, J. C., Colland, F., and Guedat, P. (2010) Synthesis and biological evaluation of 9-oxo-9H-

indeno[1,2-b]pyrazine-2,3-dicarbonitrile analogues as potential inhibitors of deubiquitinating enzymes, *ChemMedChem 5*, 552-558.

[17] Kapuria, V., Peterson, L. F., Fang, D., Bornmann, W. G., Talpaz, M., and Donato, N. J. (2010) Deubiquitinase inhibition by small-molecule WP1130 triggers aggresome formation and tumor cell apoptosis, *Cancer Res 70*, 9265-9276.

[18] Lee, B. H., Lee, M. J., Park, S., Oh, D. C., Elsasser, S., Chen, P. C., Gartner, C., Dimova, N., Hanna, J., Gygi, S. P., Wilson, S. M., King, R. W., and Finley, D. (2010) Enhancement of proteasome activity by a small-molecule inhibitor of USP14, *Nature 467*, 179-184.

[19] Wrigley, J. D., Eckersley, K., Hardern, I. M., Millard, L., Walters, M., Peters, S. W., Mott, R., Nowak, T., Ward, R. A., Simpson, P. B., and Hudson, K. (2011) Enzymatic characterisation of USP7 deubiquitinating activity and inhibition, *Cell Biochem Biophys 60*, 99-111.

[20] Sheridan, C. (2015) Drug makers target ubiquitin proteasome pathway anew, *Nature Biotechnology 33*, 1115-1117.

[21] Popov, N., Wanzel, M., Madiredjo, M., Zhang, D., Beijersbergen, R., Bernards, R., Moll, R., Elledge, S. J., and Eilers, M. (2007) The ubiquitin-specific protease USP28 is required for MYC stability, *Nat Cell Biol 9*, 765-774.

[22] Meyer, N., and Penn, L. Z. (2008) Reflecting on 25 years with MYC, *Nature Reviews Cancer 8*, 977-990.

[23] A., A., J.I., J., and Henriksson, M. A. (2010) MYC in oncogenesis and as a target for cancer therapies, *Advances in Cancer Research 107*, 163-224.

[24] Shah, S. P., Morin, R. D., Khattra, J., Prentice, L., Pugh, T., Burleigh, A., Delaney, A., Gelmon, K., Guliany, R., Senz, J., Steidl, C., Holt, R. A., Jones, S., Sun, M., Leung, G., Moore, R., Severson, T., Taylor, G. A., Teschendorff, A. E., Tse, K., Turashvili, G., Varhol, R., Warren, R. L., Watson, P., Zhao, Y., Caldas, C., Huntsman, D., Hirst, M., Marra, M. A., and Aparicio, S. (2009) Mutational evolution in a lobular breast tumour profiled at single nucleotide resolution, *Nature 461*, 809-813.

[25] Diefenbacher, M. E., Popov, N., Blake, S. M., Schulein-Volk, C., Nye, E., Spencer-Dene, B., Jaenicke, L. A., Eilers, M., and Behrens, A. (2014) The deubiquitinase USP28 controls intestinal homeostasis and promotes colorectal cancer, *J Clin Invest 124*, 3407-3418.

[26] Zhang, L., Xu, B., Qiang, Y., Huang, H., Wang, C., Li, D., and Qian, J. (2015) Overexpression of deubiquitinating enzyme USP28 promoted non-small cell lung cancer growth, *J Cell Mol Med 19*, 799-805.

[27] Welcker, M., and Clurman, B. E. (2008) FBW7 ubiquitin ligase: a tumour suppressor at the crossroads of cell division, growth and differentiation, *Nat Rev Cancer 8*, 83-93.

[28] Vervoorts, J., Luscher-Firzlaff, J., and Luscher, B. (2006) The ins and outs of MYC regulation by posttranslational mechanisms, *J Biol Chem 281*, 34725-34729.

[29] Schulein-Volk, C., Wolf, E., Zhu, J., Xu, W., Taranets, L., Hellmann, A., Janicke, L. A., Diefenbacher, M. E., Behrens, A., Eilers, M., and Popov, N. (2014) Dual regulation of Fbw7 function and oncogenic transformation by Usp28, *Cell Rep 9*, 1099-1109.

[30] Hassiepen, U., Eidhoff, U., Meder, G., Bulber, J. F., Hein, A., Bodendorf, U., Lorthiois, E., and Martoglio, B. (2007) A sensitive fluorescence intensity

assay for deubiquitinating proteases using ubiquitin-rhodamine110-glycine as substrate, *Anal Biochem 371*, 201-207.

[31] Zhang, J. (1999) A simple statistical parameter for use in evaluation and validation of High Throughput Screening Assays, *Journal of Biomolecular Screening 4*, 67-73.

[32] Habig, M., Blechschmidt, A., Dressler, S., Hess, B., Patel, V., Billich, A., Ostermeier, C., Beer, D., and Klumpp, M. (2009) Efficient elimination of nonstoichiometric enzyme inhibitors from HTS hit lists, *J Biomol Screen 14*, 679-689.

[33] Ritorto, M. S., Ewan, R., Perez-Oliva, A. B., Knebel, A., Buhrlage, S. J., Wightman, M., Kelly, S. M., Wood, N. T., Virdee, S., Gray, N. S., Morrice, N. A., Alessi, D. R., and Trost, M. (2014) Screening of DUB activity and specificity by MALDI-TOF mass spectrometry, *Nat Commun 5*, 4763.

[34] Valero, R., Marfany, G., Gonzalez-Angalo, O., Gonzalez-Gonzalez, G., Puelles, L., and Gonzalez-Duarte, R. (1999) USP25, a Novel Gene Encoding a Deubiquitinating Enzyme, Is Located in the Gene-Poor Region 21q11.2, *Genomics 62*, 395-405.

[35] Altun, M., Kramer, H. B., Willems, L. I., McDermott, J. L., Leach, C. A., Goldenberg, S. J., Kumar, K. G., Konietzny, R., Fischer, R., Kogan, E., Mackeen, M. M., McGouran, J., Khoronenkova, S. V., Parsons, J. L., Dianov, G. L., Nicholson, B., and Kessler, B. M. (2011) Activity-based chemical proteomics accelerates inhibitor development for deubiquitylating enzymes, *Chem Biol 18*, 1401-1412.

Figures:
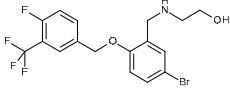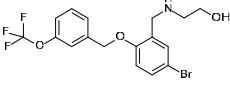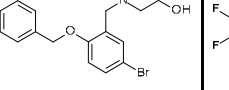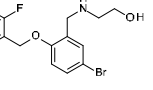
Compound Number	AZ1	AZ2	AZ3	AZ4
Structure				
USP28 IC$_{50}$ (μM) – Ub-Rh110 assay	0.7 (n = 4)	1.1 (n = 4)	59.6 (n = 3)	2.0 (n = 24)
USP28 IC$_{50}$ (μM) – Ub-TMR assay	1.0 (n = 3)	0.9 (n = 3)	68.4 (n = 3)	2.1 (n = 3)
USP28 IC$_{50}$ (μM) – tetra-Ub assay	0.8 (n = 4)	1.3 (n =4)	98.0 (n = 4)	1.5 (n = 4)
USP28 ITC K$_d$ (μM)	0.2	0.9	>100	2.7
USP28 MST K$_d$ (μM)	3.7 (n=2)	10.3 (n=2)	>100 (n=2)	3.6 (n=2)
USP25 IC$_{50}$ (μM) – Ub-Rh110 assay	0.62	0.88	52.53	Nd
USP2a IC$_{50}$ (μM) – Ub-Rh110 assay	>100 (n = 6)	>100 (n = 5)	>100	>100
Molecular Weight	422	420	336	390
LogD	3.3	3.5	2.2	2.7
LLE USP28 enzyme pIC$_{50}$-LogD	2.8	2.5	2	3
Solubility at pH$_{7.4}$ (μM)	80	166	855	652
pK$_a$	8.9	8.9	Nd	Nd
Human plasma %free	3.7	4.1	Nd	Nd

Table 1 Overall profiles of USP28/USP25 inhibitors.

The HTS hit finding approach found benzylic aminoethanols of the structural class represented by compounds AZ1-4. The *in vitro* profiles of AZ1, AZ2 and AZ4 show them to be active against the USP28 enzyme and to bind to USP28 by iso-thermal calorimetry (ITC) & Microscale Thermophoresis (MST). They were also shown to be selective over USP2a. A fourth analogue (AZ3) was shown to be significantly less potent at inhibiting USP28 but retained selectivity over USP2a. The data shown in the table were generated from one experimental replicate, unless stated otherwise.

Figure 1: Orthogonal hit validation and characterisation
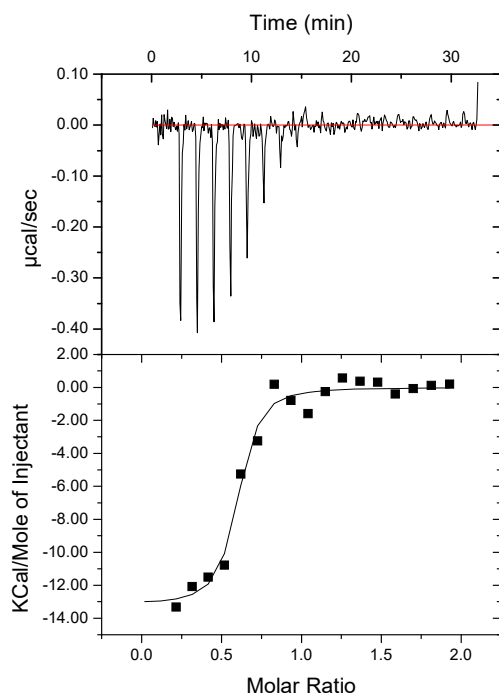
(a)   Isothermal Calorimetry: AZ1
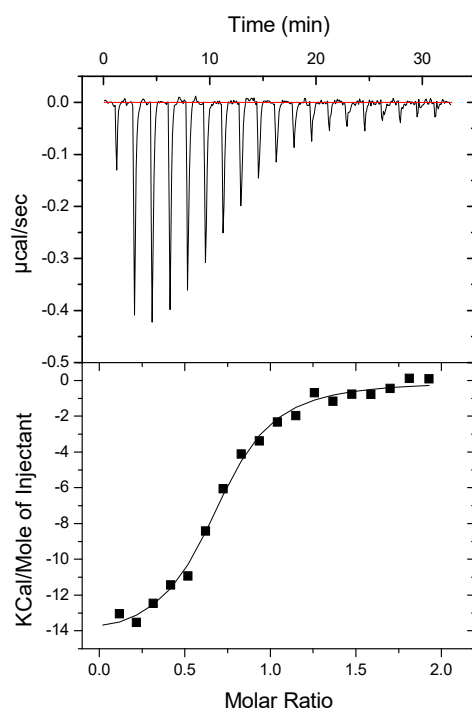

(b)   Isothermal Calorimetry: AZ2
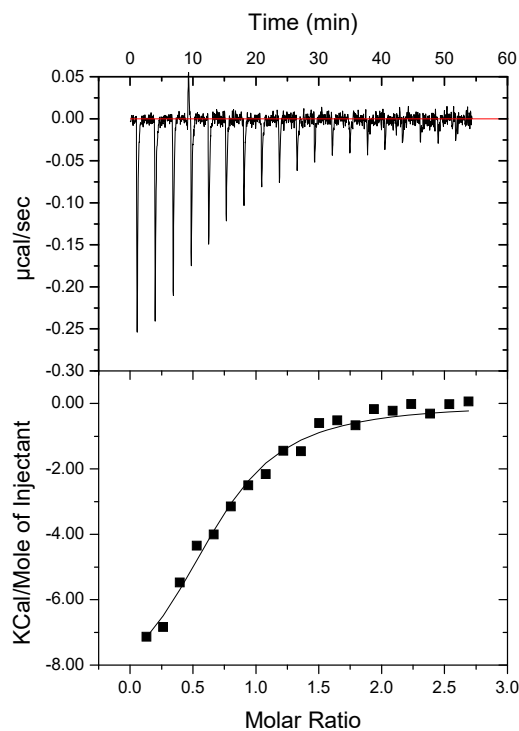
(c)   Isothermal Calorimetry: AZ4

Figure 1 a-c: Iso-thermal titration calorimetry (ITC) data demonstrating AZ1, AZ2 & AZ4 inhibitor binding to USP28. ITC ligand binding measurement confirmed inhibitor binding to USP28 and determined the affinity of the interaction. Data are shown for (a) AZ1, (b) AZ2 and (c) AZ4 binding to USP28. The less potent analogue, AZ3, failed to produce a measurable K_d value. The data shown are representative data from a single experiment. The USP28 protein and test compound binding partners were dialysed in 40 mM HEPES (pH 7.5), 150 mM NaCl, in order to minimise heat effects due to buffer mismatch or ionisation. Data was analysed using non-linear least squares regression using Microcal Origin software (GE Healthcare).

Figure 2: Inhibitor Selectivity Profiling
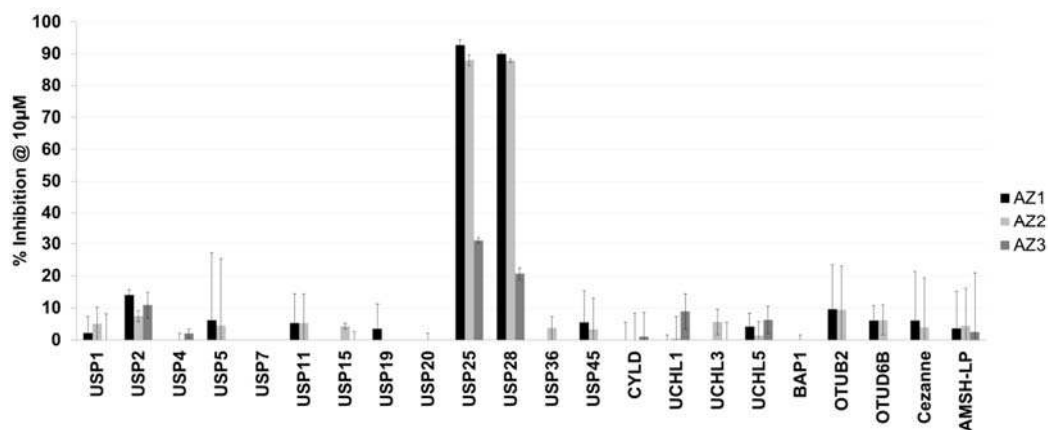
(a) **Selectivity profiling of USP28 inhibitors across DUB family members**.
Compound activity was analysed against a range of DUB family members, in the DUBProfiler panel (Ubiquigent) of purified enzyme assays using Ubiquitin-Rhodamine110 as substrate (28). Data is shown as a percentage of inhibition of the total enzyme activity for each enzyme in the panel, in the presence of 10 μM test compound. Error bars represent the standard deviation of 3 replicates.

(b)

(c)

(d)
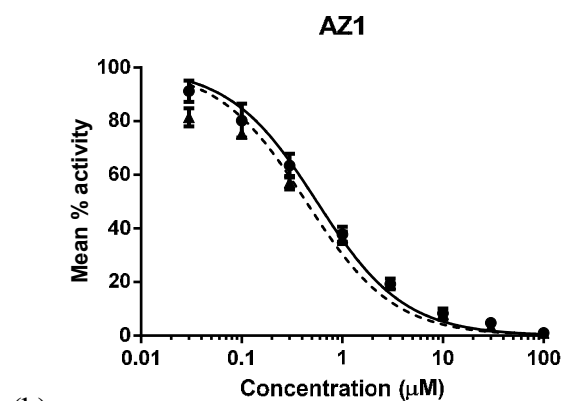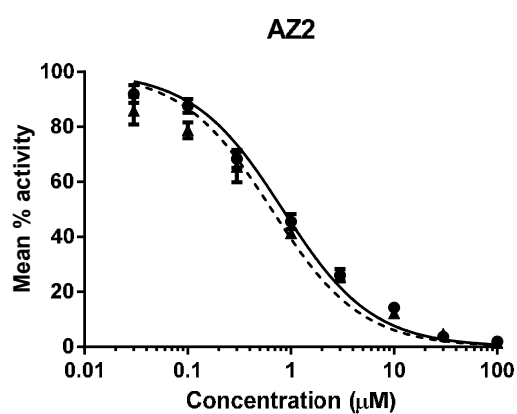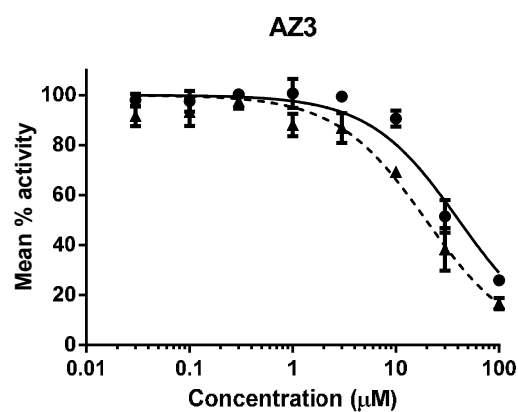
	USP25 IC$_{50}$ (μM)	USP28 IC$_{50}$ (μM)
AZ1	0.7	0.6
AZ2	0.9	0.9
AZ3	26.4	52.5

(e)

Figure 2(b-e): Dose response profiling of inhibitors against USP25 & USP28.

Compound activity was analysed against USP25 & USP28, in the DUBProfiler (Ubiquigent) purified enzyme assays using Ubiquitin-Rhodamine110 as substrate. Data is shown as a mean percentage activity at each concentration tested, thereby generating dose-response curves for (b) AZ1, (c) AZ2, and (d) AZ3. Error bars represent the standard deviation of 4 replicates. IC$_{50}$ values calculated from the dose response curves are shown in the associated table (e).

Figure 3: Cellular target engagement profiling of inhibitors
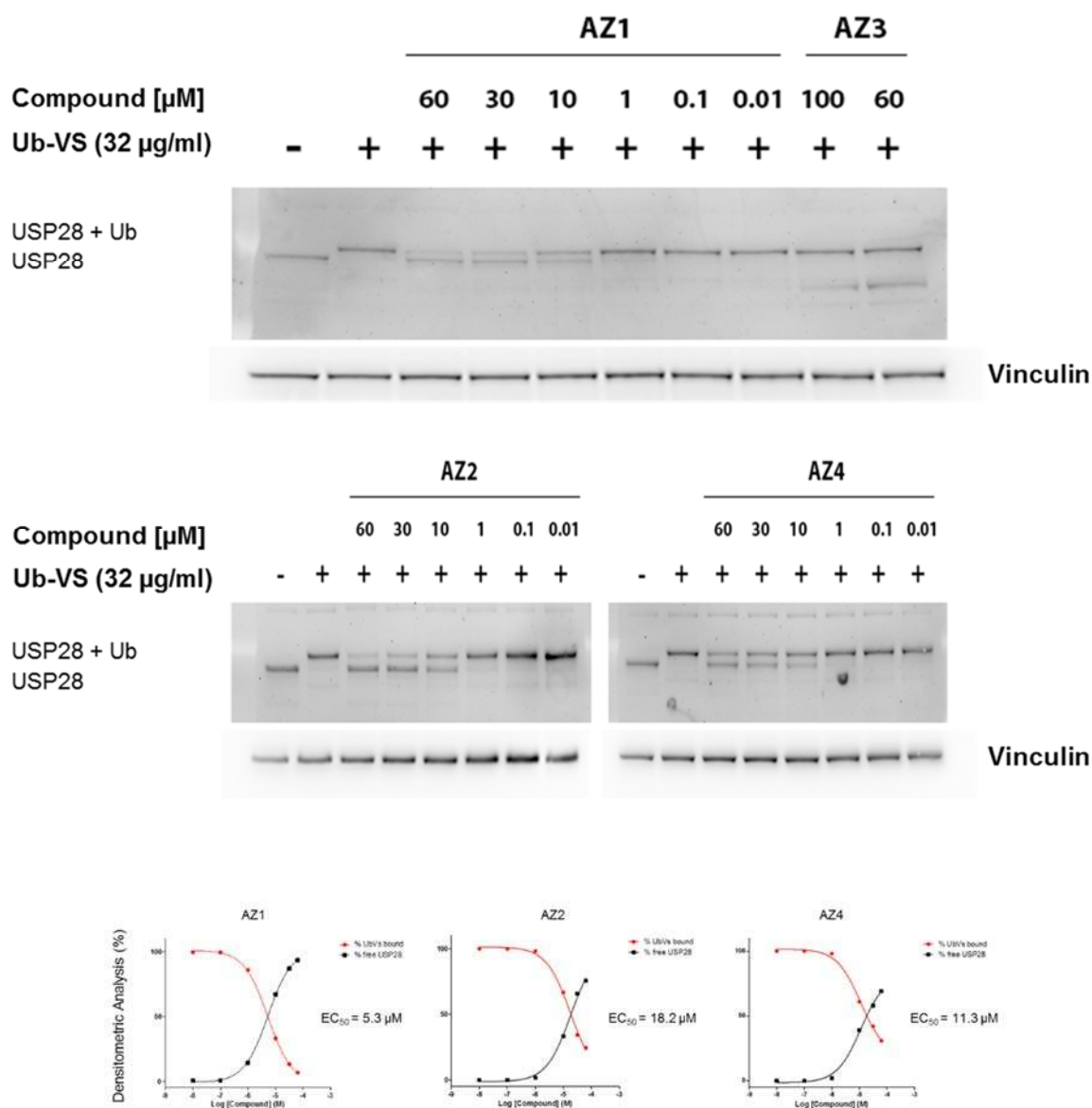
Compound	AZ1	AZ2	AZ3	AZ4
EC$_{50}$ (µM)	5.3 +/- 2.1	18.2 +/- 5.2	>100	11.3 +/-3.1

(a) Target engagement of USP28 in a cellular environment by USP28 inhibitors. HCT116 cells were treated with USP28 inhibitors at the indicated concentrations for 2 hrs. Cells were washed thrice, lysed and the Ub-VS probe added to the extract. Samples were analysed by immunoblotting probing for USP28. Upper band (USP28-Ub covalent adduct). Data presented as mean of 3 independent experiments. Quantitation by densitometry analysis was

performed on both the upper (enzyme + Ub) and lower bands (enzyme only). The data were fitted to a sigmoidal curve using GraphPad Prism (GraphPad Software, Inc, La Jolla, CA).
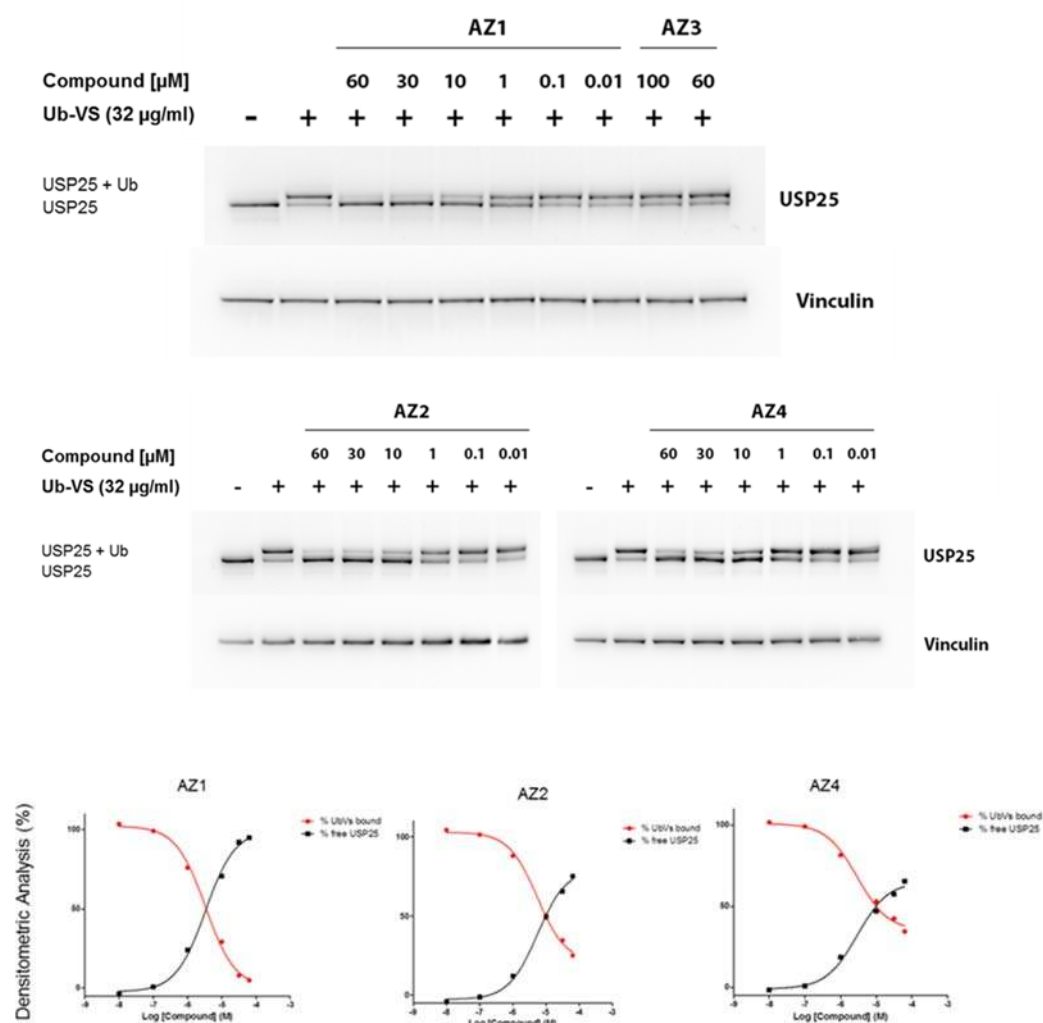
| Compound	AZ1	AZ2	AZ3	AZ4
EC$_{50}$ (µM)	3.3 +/-1.2	11.5 +/- 4.5	>100	19.6+/-3.2

(b) USP28 inhibitors engage with USP25 in a cellular context

HCT116 cells were treated with USP28 inhibitors at the indicated concentrations for 2 hrs. Cells were washed thrice, lysed and the Ub-VS probe added to the extract. Samples were analysed by immunoblotting probing for USP25. The higher bands show USP-Ub covalent adducts, demonstrating target engagement with USP25. Data presented as mean of 3 independent experiments.
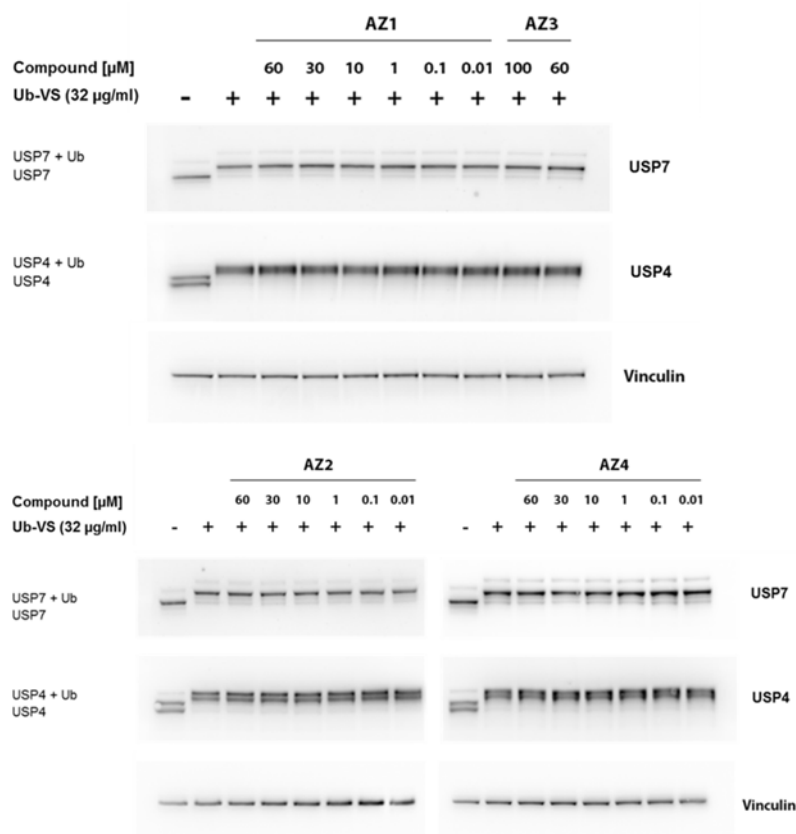
(c) USP28 inhibitors do not engage with USP7 or USP4 in a cellular context

HCT116 cells were treated with USP28 inhibitors at the indicated concentrations for 2 hrs. Cells were washed thrice, lysed and the Ub-VS probe added to the extract. Samples were analysed by immunoblotting probing for USP7 & USP4. The higher bands show USP-Ub covalent adducts, with no demonstrable target engagement with either USP7 or USP4. Data presented as mean of 3 independent experiments.

Figure 4: Phenotypic profiling of inhibitors
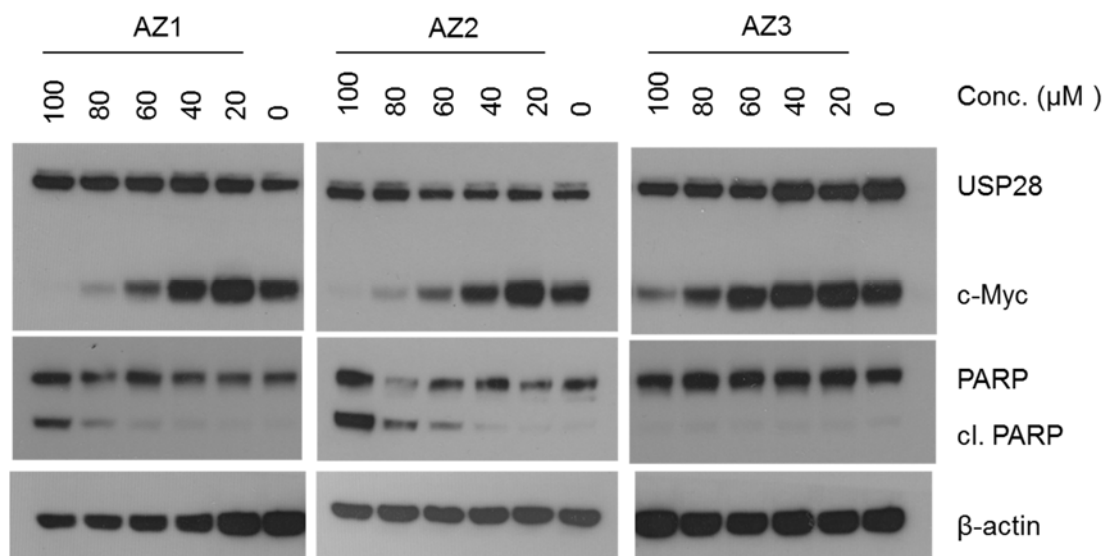
(a) **Modulation of endogenous total c-Myc levels by USP28 inhibitors.**

HCT116 cells were treated with compounds (as indicated) and samples collected after 3 hrs for Western blot analysis probing for USP28, c-Myc and PARP. β-actin was included as loading control. Full-length PARP (116 kDa), cleaved PARP (cl. PARP, 85 kDa). These data are representative data from at least 3 independent experiments. Similar observations were also made in additional cell lines including SW480 and HT29 (see Fig. S3a-b)
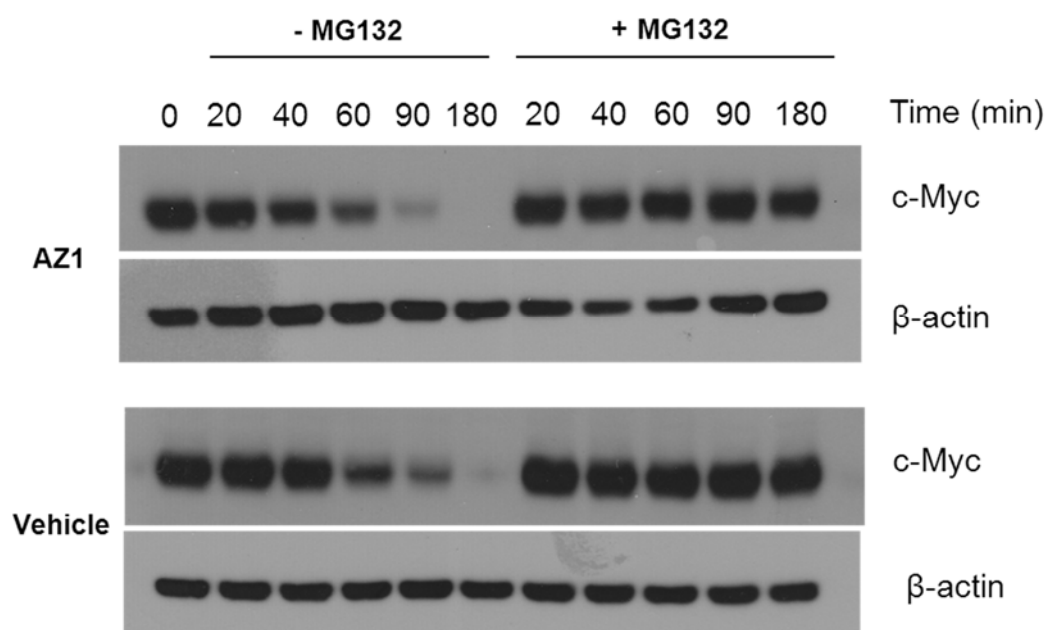
(b) **USP28 inhibitor-induced c-Myc degradation is mediated by the proteasome.** Representative data shown with AZ1. HCT116 cells were pretreated with cycloheximide (100 μg/mL) and the proteasome inhibitor MG132 (20 μM) and subsequently exposed to AZ1 (60 μM) or vehicle control (DMSO). Cells were lysed at the indicated timepoints (from 0 to 180 min) and samples analysed by Western blotting probing for c-Myc. The half-life values of c-Myc were determined by densitometry analysis based on these blots. β-actin was included as loading control. These data are representative data from at least 3 independent experiments.

Figure 5: Representative cell cycle and viability assays in HCT116 and viability data across a panel of cell lines including normals.
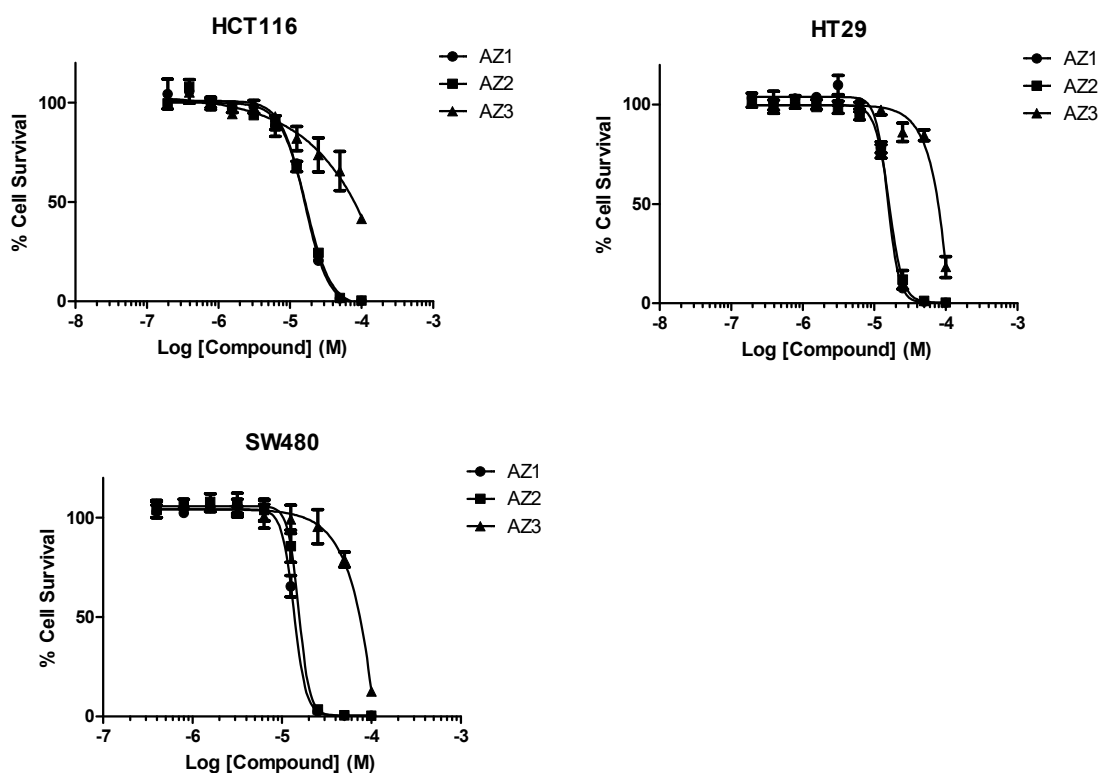
(a) **Cell viability assays** - Cells were typically seeded in 96 well plate format (typically 4000-6000 cells/well) and treated after 24 hrs with increasing concentration of compound from 0 to 100 μM in ½ log unit increments. Cell viability was assessed after 72 hrs by CellTiter-Glo® as recommended by the manufacturer's instructions (Promega). Analysis and EC$_{50}$ values were derived using GraphPadPrism (GraphPad Software, Inc, La Jolla, CA; four-parameter logistic function). Data presented as mean of at least three independent experiments. EC$_{50}$ values compiled in Supplementary Table 1.
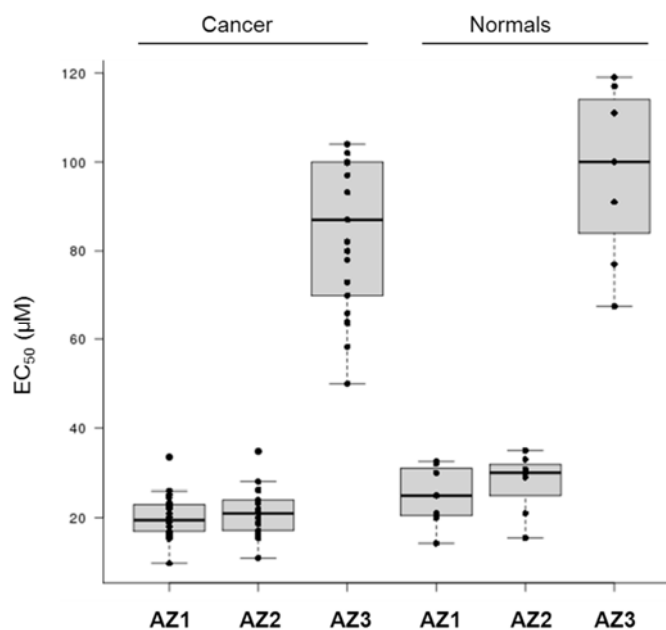
(b) **Representative viability assays in a panel of cancer and tissue-matched normal cell lines.**

Compiled EC_{50} values in normal and cancer cell lines. Proliferation assays were run as described previously using a panel of cancer (n=21) and normal cell lines (n=7) from different tissues of origin. EC_{50} values were derived using GraphPad Prism (GraphPad Software, Inc, La Jolla, CA) from at least two independent experiments. Cell line panel composition and EC_{50} values are available in Supporting information. The box plot representation was performed using R+GG plot2 package. The tick band indicates the median, the box indicates the upper and lower quantiles, the vertical line indicates the variability and the individual dots represent the various cell lines. Details on the panel composition and EC_{50} values are shown in Supplementary Table 1.

Title:

Identification and characterisation of dual inhibitors of the USP25/28 Deubiquitinating enzyme subfamily.

Authors:

Jonathan D. Wrigley[a*#], Gerald Gavory[c#], Iain Simpson[b], Marian Preston[a], Helen Plant[a], Jenna Bradley[a], Anne U. Goeppert[a], Ewelina Rozycka[c], Gareth Davies[a], Jarrod Walsh[a], Andrea Valentine[c], Keeva McClelland[c], Krzysztofa Ewa Odrzywol[c], Jonathan Renshaw[a], Joanna Boros[a], Jonathan Tart[a], Lindsey Leach[a], Thorsten Nowak[b], Richard A. Ward[b], Timothy Harrison[c] & David M Andrews[b]

#Joint Co-authors

Supplementary Information

Supplementary Methods:

Expression and purification of USP28

The extended catalytic domain of the USP28 (E147-L652) LE-6his was expressed in the BL21*(DE3) *E.coli* transformed with pET29b vector grown in Terrific broth. 21 hours post induction the grow was harvested by centrifugation. The cell pellets were resuspended 1g per 10 ml in lysis buffer of 20 mM Hepes pH8.0, 0.15 M NaCl, 5 mM 2-mercaptoethanol, 10 mM Imidazole containing Complete–EDTA free protease inhibitors (Roche) and 50 µg/ml lysozyme. Lysis was performed by sonication on ice and clarified by centrifugation. The supernatant was applied to a Nickel-NTA superflow (Qiagen) column equilibrated into 20 mM Hepes (pH8.0), 0.15 M NaCl, 5 mM 2-mercaptoethanol, 10 mM Imidazole. After loading the column was washed to remove unbound with the same running buffer. The tagged protein was eluted using this buffer containing 250 mM imidazole. The elution fractions were pooled and concentrated using a cleaned Amicon Ultra-15 centrifugal filter with a 10,000 MWCO membrane (Millipore). The pool was loaded onto a Hiload Superdex 200 16/60 prep grade (GE Healthcare) equilibrated into 25 mM Bis-Tris (pH7.0), 0.1 M NaCl, 4 mM TCEP storage buffer. The pure USP28 pool was concentrated further, aliquoted and snap frozen for storage.

***In vitro* deubiquitination assays using Ubiquitin-Rhodamine 110**

Assay Reagents

Ubiquitin-Rhodamine 110 was from Boston Biochem. All other chemicals were supplied from Sigma-Aldrich.

Assay buffer

All reactions were performed at room temperature in freshly prepared assay buffer containing 50 mM Hepes (pH 7.4), 0.5 mM EDTA, 1 mM tris-(2-Carboxyethyl) phosphine (TCEP) and 1 mg/ml bovine serum albumin.

Compound Preparation

Compounds were acoustically dispensed into black 1536-well non-binding microplates (Greiner Bio-One, UK) using an Echo 555 (Labcyte Inc., Sunnyvale, CA). For primary screening, 10 nL of 10 mM compounds solubilized in DMSO were dispensed acoustically into the wells. This gave a final concentration of 0.3% (v/v) DMSO and a final in-well compound concentration of 33.3 μM after addition of all reagents. For concentration-response screening, varying amounts of compound were dispensed acoustically to give a doubling dilution range. Wells were backfilled with the required volume of DMSO to ensure a final concentration of 1% (v/v) after addition of all reagents.

Assay Optimization

Cleavage of the rhodamine Ubiquitin-Rhodamine 110 was confirmed by incubating 80 nM Ubiquitin-Rhodamine 110 in assay buffer with 0.25 nM USP28 in a final volume of 6 μL. The fluorescence signal was read every 5 minutes for 35 min. The effect of different reductants on enzyme activity was determined by incubating 80 nM Ubiquitin-Rhodamine 110 with 0.25 nM USP28 in assay buffer containing either 1 mM dithiothreitol (DTT), glutathione or TCEP. Kinetic parameters for the USP28-catalyzed cleavage of nM Ubiquitin-Rhodamine 110 were determined by incubating varying concentrations of Ubiquitin-Rhodamine 110 with 0.25 nM USP28. The fluorescence signal was read on a Pherastar microplate reader (BMG Labtech, Ortenberg, Germany) using excitation 485 nm, emission 520 nm, every minute for 30 min. Initial rate data were fitted to the Michaelis-Menten equation using GraphPad Prism V.5 (GraphPad Software Inc.).

Inhibition of USP28 by Ubiquitin aldehyde

0.25 nM USP28 in assay buffer was incubated with varying concentrations of Ubiquitin aldehyde. These were incubated at room temperature for 20 minutes, prior to the addition of 80 nM Ubiquitin-Rhodamine 110. The plates were covered and left to incubate for a further 30 mins at room temperature. 100 mM citric acid was added before measuring fluorescence as before. The IC_{50} data were fitted using GraphPad Prism (GraphPad Software, La Jolla, CA).

High throughput screen for USP28 inhibitors

Test compounds from the AstraZeneca compound collection were dissolved in DMSO to form stock solutions (10 mM). A final concentration of 0.3% v/v of DMSO and 10 µM test compound was achieved after reagent additions. An Innovadyne Nanodrop (PAA, Colorado) was used to dispense 1.5 µL of 0.5 nM USP28 in assay buffer (50 mM Hepes (pH 7.5), 0.5 mM EDTA, 0.1 mg/ml BSA, 1 mM TCEP) to assay plates containing compound, before briefly centrifuging the plates at 150 g for 10 seconds in a Vspin (Agilent, Santa Clara, CA). After 20 minutes incubation at room temperature, 1.5 µL of 160 nM Ubiquitin-Rhodamine 110 in assay buffer was added using a Nanodrop and the plates centrifuged as before. The reaction was incubated at room temperature for 30 minutes, before the addition of 1.5 µl of 100 mM citric acid using a Latitude (Deerac Fluidics, Sunnyvale, CA) to stop the reaction. Fluorescence signal was measured as before.

Concentration Response Follow-up Screening

8-point, doubling dilution concentration-response curves, with a top concentration of 100 µM were constructed. The assay was performed using the process described for the high-throughput compound library screening. Assay using the tetra-ubiquitin Rh110 substrate (tetra-Ub Rh110 K63-linked; # UC355; Boston Biochem) was performed as described above for the Ub-Rh110 substrate using commercially available USP28 (Boston biochem, # E-570). The fluorescence polarisation (FP) assay was performed as described above using instead the isopeptide ubiquitin-Lys-tetramethylrhodamine substrate (Ub-TMR; U-558, Boston Biochem). FP was measured every 15 min over a period of 90 min (within the linear range of the assay) using a Synergy 4 plate reader (BioTek) exciting at 530 nm and measuring the amount of parallel and perpendicular light at 575 nm. The FP signal was subsequently normalised to the no compound control (i.e. DMSO). Analysis and IC_{50} values were derived using GraphPadPrism (GraphPad Software, Inc, La Jolla, CA; four-parameter logistic function). All data presented as mean ± s.d. (n >=3).

Mode of inhibition study

AZ1 at final assay concentrations ranging from 200 nM to 5 µM was pre-incubated for 30 min with 1.5 nM of full-length USP28 (0.5 nM final assay concentration). Five

microliters of tetra-ubiquitin substrate (Tetra-Ub K63-linked; 100 nM to 40 µM to a final assay volume of 15 µl in low volume black 384-well plates (Greiner # 784076). Fluorescence intensity (ex = 487-14 nm, em = 535-30 nm) was measured over 90 min using a CLARIOstar plate reader (BMG LABTECH) and initial linear rates were calculated. Global fit analysis for competitive models were performed using GraFit (Leatherbarrow, R.J. (2001) GraFit Version 5, Erithacus Software Ltd., Horley, U.K.;Global fit Michaelis-Menten enzyme inhibition).

Data analysis
HTS data were analyzed using proprietary AstraZeneca software.

Reversibility studies
For the high-dilution assay, USP28 was pre-incubated for 30 min with 10x the inhibitor IC_{50} value followed by 100x dilution. USP28 activity was assessed 15 min post-dilution as described above. Iodoacetamide (Sigma-Aldrich; #A3221) was used as a positive control for this experiment at a final pre-dilution concentration of 1.0 mM. Data analysis was performed as described previously.

"Ratio test" assay
8-point, doubling dilution concentration-response curves, with a top concentration of 100 µM were constructed. The assay was performed using the process described for the high-throughput compound library screening. A further assay was performed on the same set of compounds using a concentration of 5 nM USP28 and an incubation time of 3 minutes.

Binding Assays – Nanotemper
20 µM USP28 was labeled with a red fluorescent dye (NT-647) using Monolith NT ™ Protein Labelling Kit RED (NanoTemper Technologies GmbH, Munich, Germany). Phosphate buffered saline (PBS) containing 0.4 mM TCEP and 0.3 % (v/v) Tween-20 was used as the assay buffer for compound and protein dilutions. Compounds were serially diluted in doubling dilutions to generate 16-point concentration ranges with final assay concentrations between 100 µM and 0.003 µM. Labelled USP28 was diluted to a final assay concentration of 50 nM. 20 µl of diluted compound was mixed with 20 µl of diluted fluorescently labelled protein and

incubated under ambient conditions for 30 minutes. Each compound / protein mixture was spun for 5 minutes at 13,000 rpm prior to aspiration into a glass capillary to minimise uptake of aggregated particulate. 16 samples could be analysed within one MST experiment. The utilisation of hydrophilic glass capillaries was necessary due the propensity of USP28 to bind to untreated glass surfaces. Analysis was performed on a Monolith NT using the following settings: Infra-red laser power at 25 %, laser on time (heating) = 30 seconds, laser off time (cooling) = 5 seconds. The data were normalised against the baseline obtained in the absence of any inhibitor, and the maximal response obtained at the highest concentration of inhibitor. The (dissociation constant) (K_d) was calculated by plotting delta Fnorm (shift in normalised fluorescence) against the logarithm of the compound dilution series concentrations. The resulting sigmoidal binding curve could be directly fitted with a non-linear solution of the law of mass action. All experiments were performed with a minimum of 3 replicates and the delta Fnorm curves analysed using Origin software (OriginLab Corporation, Northampton, MA, USA).

Flow cytometry

Cells were plated in 6 cm dish ($2.5x10^5$ cells/well) and treated with compounds as indicated. Cells (including floating cells) were collected after 24 or 48 hrs, rinsed with PBS/FCS (1%, v/v) and fixed with 70% EtOH and kept at 4°C until needed. Cells were subsequently stained with Propidium Iodide solution (100 µg/mL PI in 1x PBS) and incubated at RT for 30 min. Cell cycle analysis was performed using flow cytometry (FACSalibur) and the CellQuest Software.

Chemistry:

Compounds AZ1-4 were prepared as described below.

2-(5-Bromo-2-(4-fluoro-3-(trifluoromethyl)benzyloxy)benzylamino)ethanol, **AZ1**
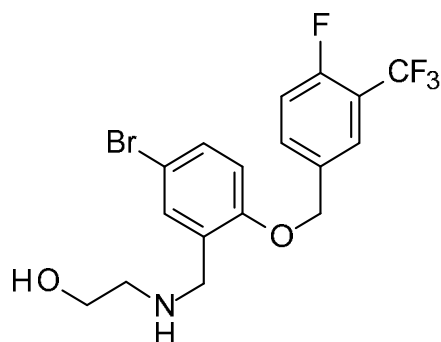
Potassium carbonate (2.75 g, 19.90 mmol) was added to 4-(bromomethyl)-1-fluoro-2-(trifluoromethyl)benzene (2.81 g, 10.94 mmol) and 5-bromo-2-hydroxybenzaldehyde (2 g, 9.95 mmol) in DMF (50 mL) at 20 °C under nitrogen. The resulting yellow suspension was stirred at 20 °C for 16 hrs. The reaction mixture was then poured into ice water, the resulting white precipitate filtered, washed with copious water and dried under vacuum to give 5-bromo-2-(4-fluoro-3-(trifluoromethyl)benzyloxy)benzaldehyde (3.61 g, 96 %) as a white solid. 2-aminoethanol (0.922 mL, 15.27 mmol) was added to 5-bromo-2-(4-fluoro-3-(trifluoromethyl)benzyloxy)benzaldehyde (1.44 g, 3.82 mmol) in THF (35 mL) with acetic acid (2 drops) added under nitrogen. The solution was then stirred for 10 mins. Sodium triacetoxyhydroborate (2.428 g, 11.45 mmol) was then added portionwise over 30 minutes and the resulting suspension was stirred at 20 °C for 16 hrs. The reaction mixture was then poured onto 10% NaHCO$_3$ solution (200 mL) and the aqueous phase was extracted with ethyl acetate (2 x 200 mL). The combined organic phases were dried over Na$_2$SO$_4$, filtered and evaporated to give a yellow gum. The crude product was purified by flash silica chromatography, elution gradient 0 to 10% MeOH in DCM. Pure fractions were combined and evaporated to dryness to afford 2-(5-bromo-2-(4-fluoro-3-(trifluoromethyl)benzyloxy)benzylamino)ethanol (1.23 g, 76%) as a white solid. ^{1}H NMR (400 MHz, D$_6$-DMSO, 22 °C) 2.17 (1H, s), 2.55 (2H, t), 3.44 (2H, dt), 3.70 (2H, s), 4.48 (1H, t), 5.20 (2H, s), 7.01 (1H, d), 7.38 (1H, dd), 7.46 - 7.65 (2H, m), 7.75 - 8 (2H, m) ppm; 13C-NMR (176 MHz, D$_6$-DMSO, 22 °C) 46.90, 51.11, 60.36, 67.98, 112.39, 114.14, 116.47 (dq, J=32.17, 12.91), 117.31 (d, J=20.38), 122.51 (q, J=271.87), 125.97 – 126.11 (m), 129.94, 131.18, 132.02, 134.08, 134.13, 154.86, 158.31 (d, J=254.92); HRMS +ESI *m/z* calc. for [M+H]$^+$ C$_{17}$H$_{17}$O$_2$NBrF$_4$ 422.03733, found 422.03738.

2-(5-bromo-2-(3-(trifluoromethoxy)benzyloxy)benzylamino)ethanol, **AZ2**
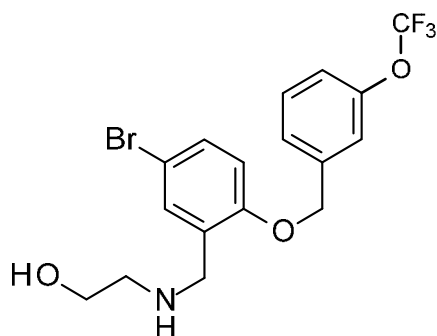
Potassium carbonate (2.75 g, 19.90 mmol) was added to 1-(bromomethyl)-3-(trifluoromethoxy)benzene (2.79 g, 10.94 mmol) and 5-bromo-2-hydroxybenzaldehyde (2.000 g, 9.95 mmol) in DMF (50 mL) at 20°C under nitrogen. The resulting yellow suspension was stirred at 20 °C for 16 hrs. The reaction mixture was poured into ice water, the resulting white precipitate filtered off, washed with water and dried under vacuum at 50° C. At this temperature, the product melted. The liquid was then dissolved in DCM, passed through phase separating cartridge and filtrate concentrated under reduced pressure to give 5-bromo-2-(3-(trifluoromethoxy)benzyloxy)benzaldehyde (1.682 g, 45.1 %) as a pale yellow liquid that crystalised on standing to an off-white solid. 2-Aminoethanol (1.081 mL, 17.91 mmol) was added to 5-bromo-2-(3-(trifluoromethoxy)benzyloxy)benzaldehyde (1.680 g, 4.48 mmol) in THF (50 mL) with acetic acid (few drops) added under nitrogen. The solution was stirred for 10 mins. sodium triacetoxyhydroborate (2.85 g, 13.44 mmol) was then added portionwise over 30 minutes and the resulting suspension was stirred at 20 °C for 2 hrs. Reaction did not look to be progressing by TLC so heated to 50°C for 16 hrs. The reaction mixture was poured onto 10% $NaHCO_3$ solution (200 mL) and extracted with ethyl acetate (2 x 200 mL). The organics were dried over Na_2SO_4, filtered and evaporated to give a yellow gum. The crude product was purified by flash silica chromatography, elution gradient 0 to 10% MeOH in DCM. Pure fractions were evaporated to dryness to afford 2-(5-bromo-2-(3-(trifluoromethoxy)benzyloxy)benzylamino)ethanol (1.521 g, 81 %) as a white solid. ^{1}H NMR (400 MHz, DMSO, 22°C) 2.57 (2H, t), 3.43 (2H, d), 3.72 (2H, s), 4.50 (1H, s), 5.19 (2H, s), 7.00 (1H, d), 7.26 - 7.41 (2H, m), 7.51 (4H, m) ppm; ^{13}C-NMR (176 MHz, D6-DMSO, 22 °C) 46.89, 51.14, 60.40, 68.45, 112.31, 114.09, 119.42, 120.0 (q, J=256.36) 120.11, 126.10, 129.86, 130.42, 131.08, 132.08, 139.77, 148.41, 154.89; HRMS +ESI *m/z* calc. for [M+H]$^+$ $C_{17}H_{18}O_3NBrF_3$ 420.04167, found 420.04221.

AZ3 and AZ4 were made in analogous manner to the preparations of AZ1 and AZ2 above. AZ3 and AZ4 exhibited the following analytical data:

2-{[2-(benzyloxy)-5-bromobenzyl]amino}ethanol, **AZ3**
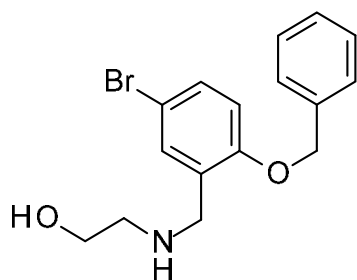
^{1}H NMR (400 MHz, DMSO, 22°C) 2.14 (1H, s), 2.55 (2H, dd), 3.46 (2H, q), 3.71 (2H, s), 4.49 (1H, t), 5.13 (2H, s), 7.01 (1H, d), 7.29 - 7.48 (6H, m), 7.50 (1H, d); ^{13}C-NMR (176 MHz, DMSO) 44.03, 48.84, 56.23, 69.88, 111.78, 114.70, 122.65, 127.52, 127.89, 128.40, 132.86, 133.73, 136.37, 155.81; HRMS ESI+ *m/z* calc. for $C_{16}H_{18}BrNO_2$, 336.05937, found 336.05978.

2-({5-Bromo-2-[(2,4,5-trifluorobenzyl)oxy]benzyl}amino)ethanol, **AZ4**
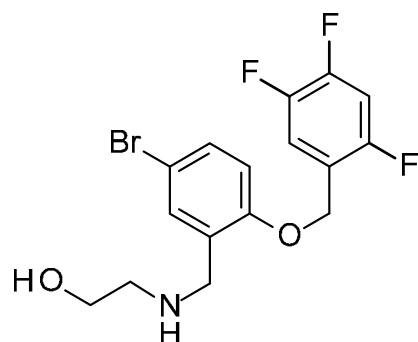
^{1}H NMR (400 MHz, DMSO, 21 °C) 2.02 (1H, s), 2.53 (2H, t), 3.44 (2H, q), 3.67 (2H, s), 4.47 (1H, t), 5.13 (2H, s), 7.07 (1H, d), 7.39 (1H, dd), 7.51 (1H, d), 7.59 7.76 (2H, m)

^{13}C-NMR (176 MHz, D_6-DMSO, 22 °C) 46.79, 51.06, 60.39, 63.11, 106.14 (dd, J = 21.4, 28.2), 112.62, 114.24, 118.08 (dd, J = 5.3, 19.9), 120.89 (dt, J = 16.4), 129.93, 131.15, 132.21, 145.98 (ddd, J=242.71, 12.72, 3.09), 149.05 (dt, J= 250.02, 13.66), 154.77, 155.50 (dd, J=245.17, 9.48); HRMS +ESI *m/z* calc. for $C_{16}H_{15}BrF_3NO_2$ [M+H]$^+$ 390.03110, found 390.03311.

Supplementary Results/Discussion:

USP28 screening and hit identification.

The Ub-Rh110 assay was chosen based on its superior optical properties to alternatives such as Ubiquitin-AMC, whose emission/excitation wavelengths (~360/~460nm) correspond to a spectrum range over which small molecule compounds typically absorb or emit, potentially resulting in assay artefacts. This strategy was also favoured based on the feasibility and simplicity of such an approach, compared to the complexities of utilising a cell-based assay for analysis of c-Myc levels, which would require significant deconvolution of hits, due to the range of additional factors that could impact on cellular c-Myc levels.

As part of our assay set-up and validation activities, initial studies were performed to determine the optimal enzyme and substrate concentrations and a suitable time course for the reaction (data not shown). The selected conditions of 80 nM Ub-Rho110 and 0.25 nM USP28 yielded linear time-dependant cleavage, and an approximately 3-fold signal : noise window at the chosen 30 minutes assay timepoint (Fig.S1a). The Michaelis-Menten parameters were determined by monitoring the rate of reaction at several different concentrations of substrate. A K_m value of 1918 ± 100 nM for Ub-Rh110 versus USP28 was determined (Fig. S1b). For comparison, this value is similar to the K_m value of 1137 ± 93 nM derived in a previous screen for USP2a. A substrate concentration of 80 nM was chosen for screening (~25-fold below the K_m value) in order to identify competitive inhibitors.

Based on previous observations with an *in vitro* Ub-AMC assay for USP7, the choice of reducing agent included in the assay may have a significant impact on both assay performance and the nature of the hits identified (12). For this reason, we performed studies to analyse the effect of several reducing agents on the assay window (Fig.S1c). This demonstrated that although a signal was obtained under all conditions, the assay window was the highest using 1 mM TCEP, which was therefore chosen for subsequent use. Another crucial step in assay validation was to demonstrate that a known inhibitor showed activity in this assay format. To this aim, Ubiquitin aldehyde (Ub-Al) was tested at a range of concentrations to generate a dose response curve, which yielded an IC_{50} value of 6.4 nM (Fig. 1Sd). Assay robustness and

reproducibility were also determined and monitored by multiple testing using Ub-Al as positive control. Assay statistical analyses demonstrated good reproducibility both within and between assays and also yielded Z′ values of around 0.8, demonstrating in turn good assay robustness (data not shown).

Assay performance was monitored throughout the campaign by means of controls for the maximum signal and 50% and 100% inhibition, to ensure reproducibility of the assay signal and inhibition. Whilst DMSO was used as a control for the maximal signal, a previously reported inhibitor of USP7 was also utilised for the inhibitory controls (Compound 1j/B, Patent: WO 2007/066200 A2). Z′ values were monitored throughout testing and values >0.7 were consistently generated throughout primary and follow-up screening (data not shown).

A primary hit rate of approximately 5.3% was obtained and the compound inhibition data yielded the expected bell-shaped distribution around a median of approximately 0% inhibition (Fig. S1e).
Based on this assay, a validation rate of 36% was obtained leading to an overall hit rate of 0.3% (15/40000) for the entire screen. Our subsequent characterisation, commencing with IC_{50} determination, focused exclusively on these likely-specific inhibitors.

Biophysical Techniques:

NanoTemper Microscale Thermophoresis (MST) was employed to confirm compound binding and this technique involved labelling of the USP28 target protein with a red fluorescent dye (NT-647) or utilised its intrinsic fluorescence. The target was then treated with a serial dilution of unlabelled compounds in a glass capillary. An infrared laser was used to generate precise microscopic temperature gradients in the capillary and the motion of fluorescently labelled molecules along these gradients is measured. Ligand binding to a target protein alters the enveloping hydration shell causing unbound and ligand-bound protein to respond differently to the thermophoretic force allowing determination of binding affinities.

Effects on Cell Cycle:

To investigate the effect of the compounds over a longer period of time, flow cytometry analysis was performed. HCT116 cells were treated with various concentrations of the compounds (typically 10, 20 and 40 µM), fixed and stained with Propidium Iodide (PI) after 24 and 48 hrs of treatment. Under the conditions of these experiments, this analysis revealed that AZ1 and AZ2 induced cell death in a dose-dependent manner as evidenced by the accumulation of a sub-G1 population. Whilst the effect was clearly noticeable at 24 hrs, apoptosis induction was particularly strong following 40 µM compound treatment after 48 h (25% *vs* >60%; Fig. S4). At lower concentrations (<20 µM), the cell cycle profiles were directly comparable to the control. No significant effects were observed on the cell cycle profiles following treatment of cells with the less active analogue AZ3 at 48 hrs (up to 40 µM).

Supplementary Figures:

Figure S1: Characterisation of USP28 *in vitro* enzyme activity, assay development and screening.
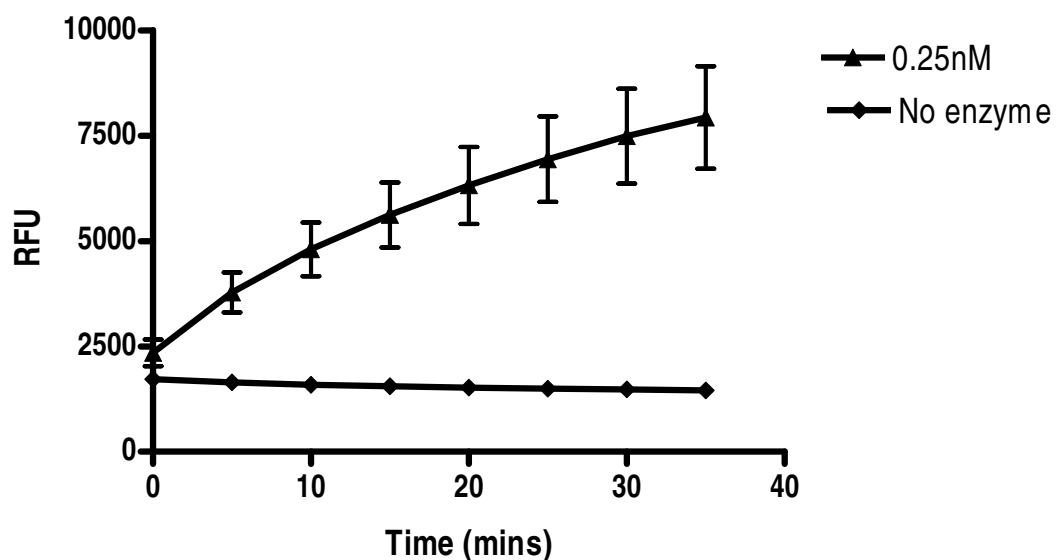

(a) **Representative reaction progress and assay signal following the cleavage of Ubiquitin-Rhodamine 110 by USP28.** Reaction time course of 80 nM Ubiquitin-Rhodamine 110 and 0.25 nM USP28. The graph shows representative data from one of three independent experiments. The data are the mean of the three replicates from that experiment and the error bars are the standard deviation of the replicates within the experiment.
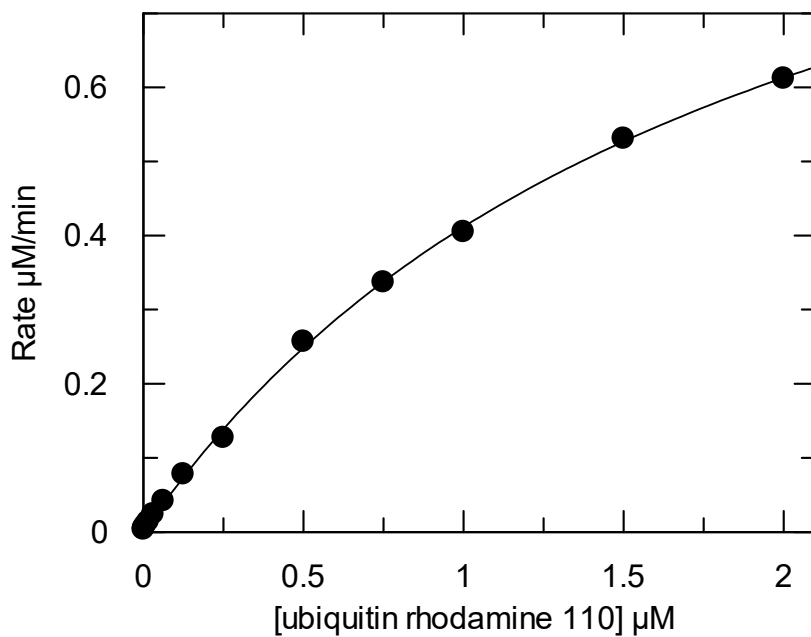
(b) **Determination of the K_m of USP28 for Ubiquitin-Rhodamine 110**. Varying concentrations of Ubiquitin-Rhodamine 110 were incubated in the presence of 0.25 nM USP28. The diagram shows the mean of n = 4 data from one of two independent experiments. The initial rate data were fitted to the Michaelis-Menten equation using GraFit V.7 (Erithacus Software, Surrey, UK), giving a K_m value of 1918 ± 100 nM.
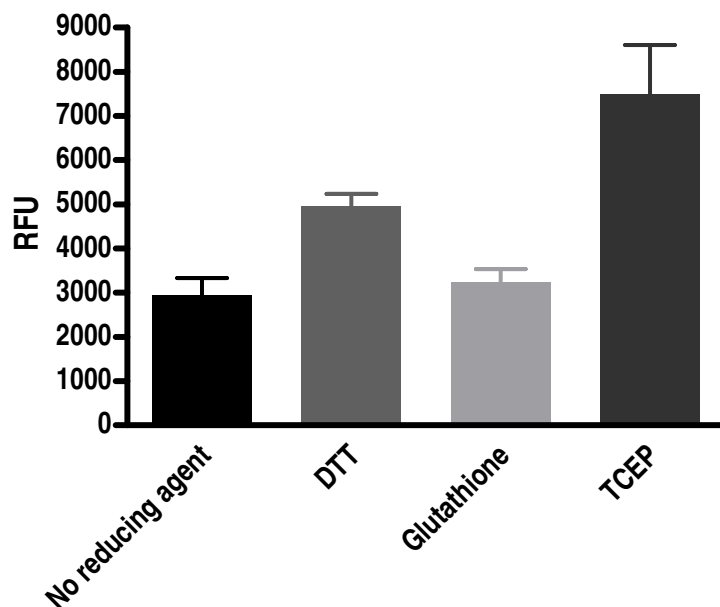
(c) **Measuring the effect of different reducing agents on USP28 activity.** 80 nM Ubiquitin-Rhodamine 110 was incubated with 0.25 nM USP28 in the presence of different reducing agents tested at 1 mM. The data shown are representative data from a single experiment. The data are the mean of four replicates from that experiment and the error bars are the standard deviation of the replicates within the experiment.
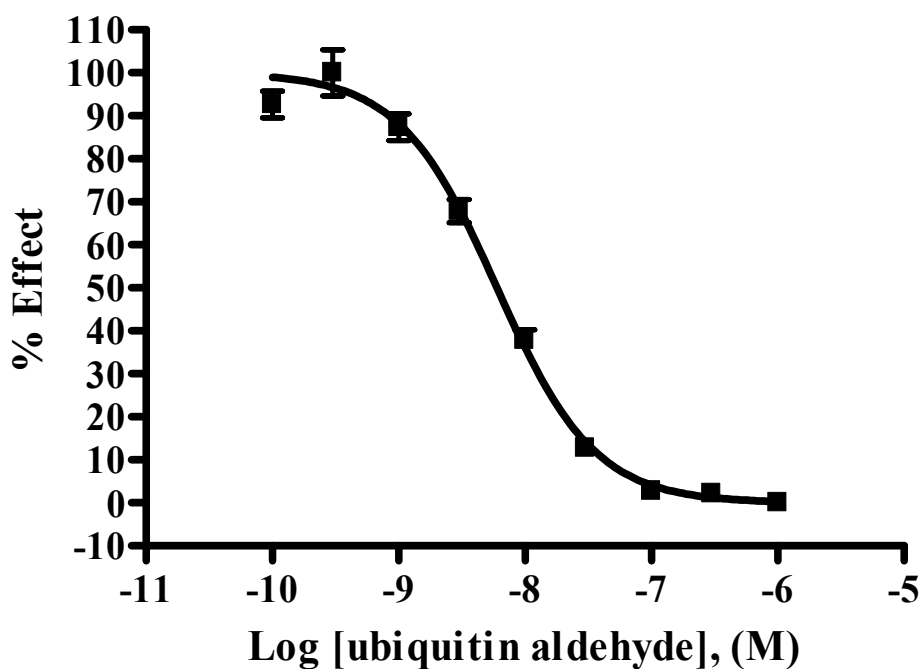
(d) **Validation of the USP28 enzyme assay with Ubiquitin aldehyde.** 80 nM Ubiquitin-Rhodamine 110 was incubated with 0.25 nM USP28 in the presence of different concentrations of Ubiquitin aldehyde (as indicated). The data shown are representative data from a single experiment. The data were fitted to a sigmoidal curve using GraphPad Prism (GraphPad Software, Inc, La Jolla, CA), giving an IC_{50} value of 6.4 nM (95% CIR 1.22). Error bars represent the standard deviation of 3 replicates.
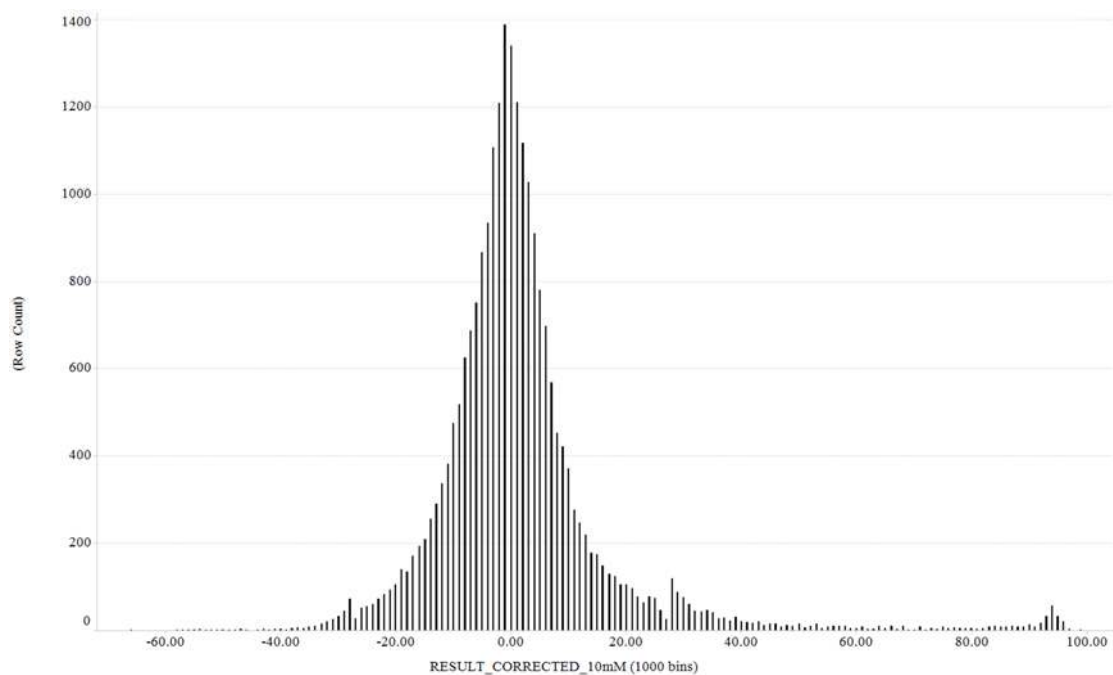
(e) **Normalised distribution of USP28 primary screen data.** The data is centred around zero. The data was analysed using proprietary AstraZeneca software and TIBCO Spotfire 5.0.1 (TIBCO Software Inc., Boston, MA).
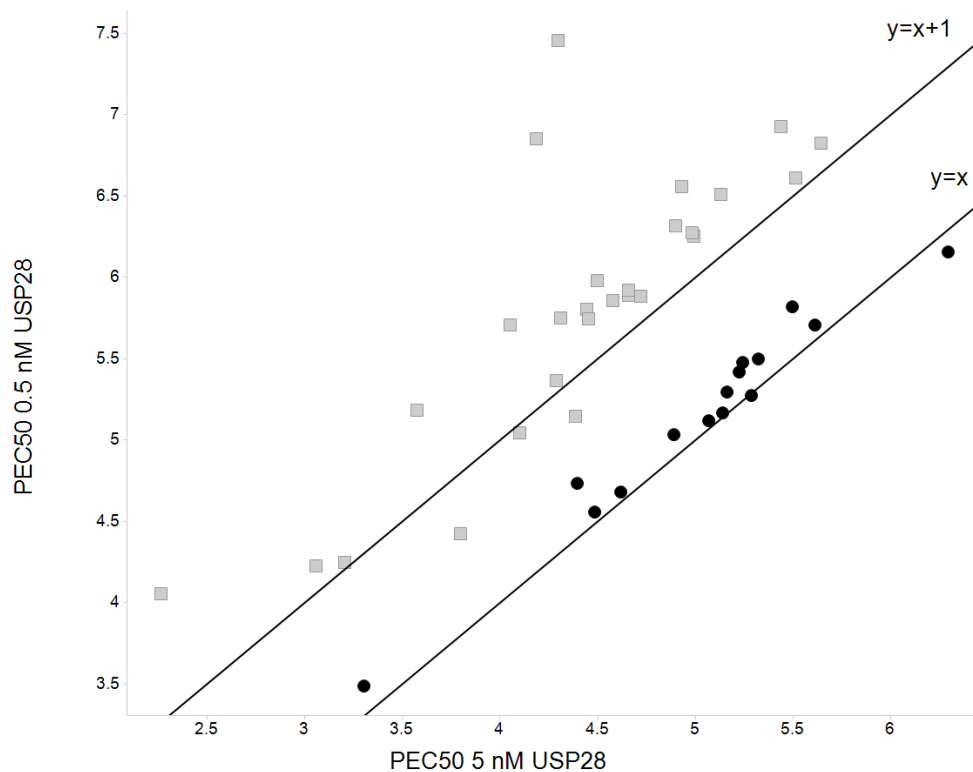
(f) **Indication of non-stoichiometric inhibition ("ratio test assay").** The data are the derived pEC50 values determined at 0.5 nM USP28, 30 min incubation (circles) and at 5 nM USP28, 3 min incubation (squares). The data was analysed using proprietary AstraZeneca software and TIBCO Spotfire 5.0.1 (TIBCO Software Inc., Boston, MA).

Compound AZ1, K_d = 3.7µM ± 1.2 µM
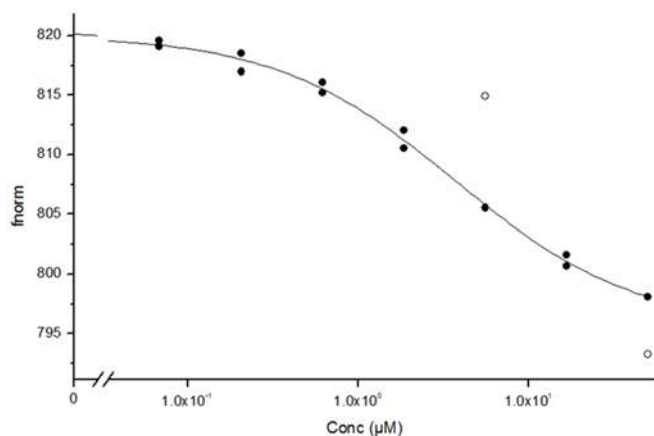
(a)   Microscale Thermophoresis: AZ1

Compound AZ2, K_d = 10.3 µM ± 4 µM
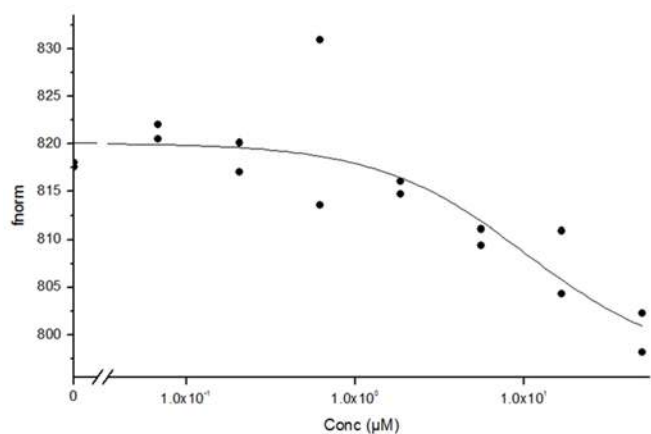
(b)   Microscale Thermophoresis: AZ2

Figure S2: Confirmation of USP28 binding by Microscale Thermophoresis (MST). Kd values were determined utilising the intrinsic fluorescence of USP28 with a 30 minutes incubation with compound for (a) AZ1 and (b) AZ2. The data presented represent two replicates within an experiment, generated on two separate experimental occasions. The data were analysed using Origin software (OriginLab Corporation, Northampton, MA, USA).
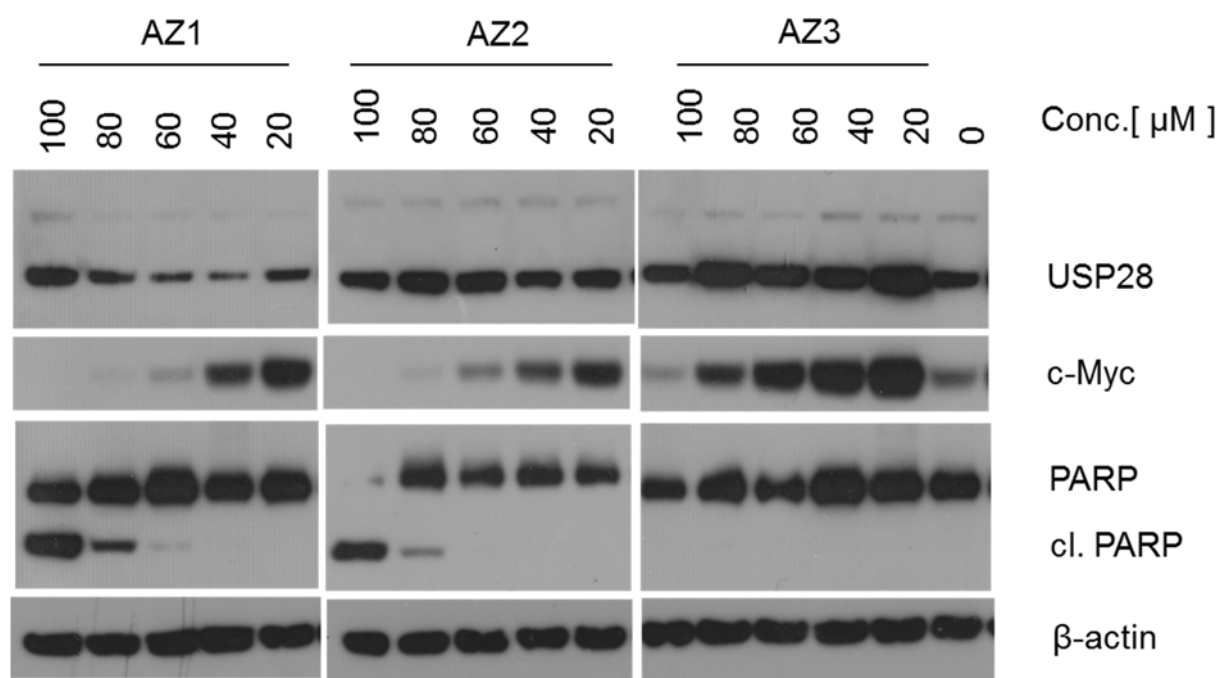
(a) SW480
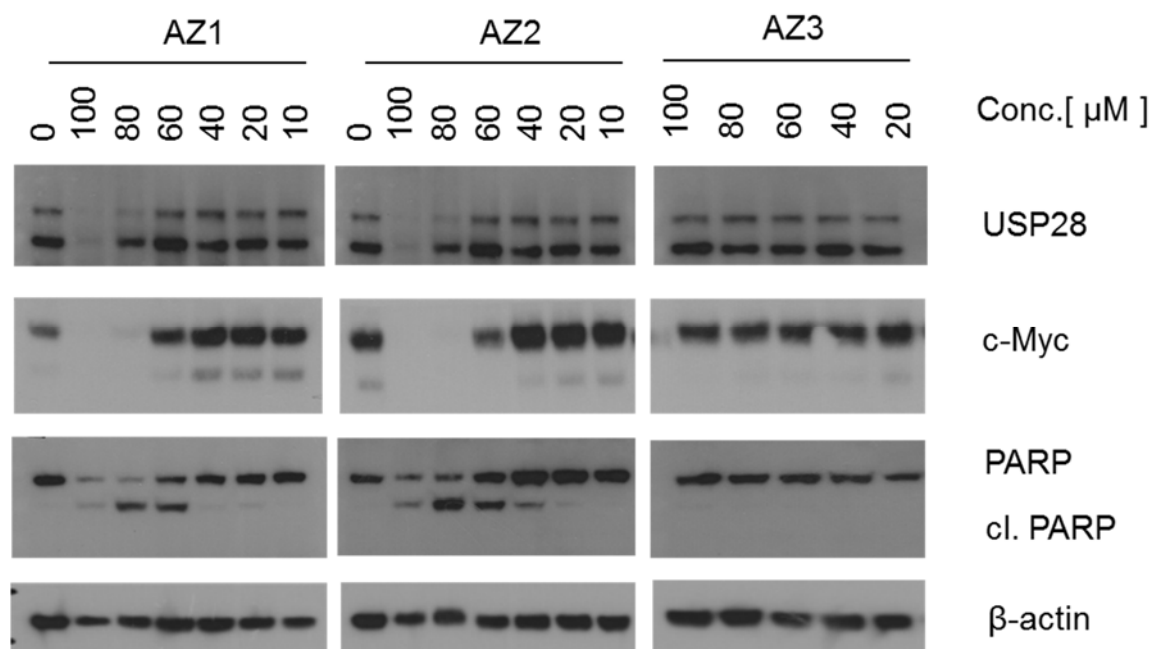
b) HT29

Figure S3 - Modulation of c-Myc levels and apoptosis induction in multiple other cell lines. (a) SW480, (b) HT29 cells were treated with compounds (as indicated) and samples collected after 3 hrs for Western blot analysis probing for USP28, c-Myc and PARP. β-actin was included as loading control. Full-length PARP (116 kDa), cleaved PARP (cl. PARP, 85 kDa). These data are representative data from at least 2 independent experiments.
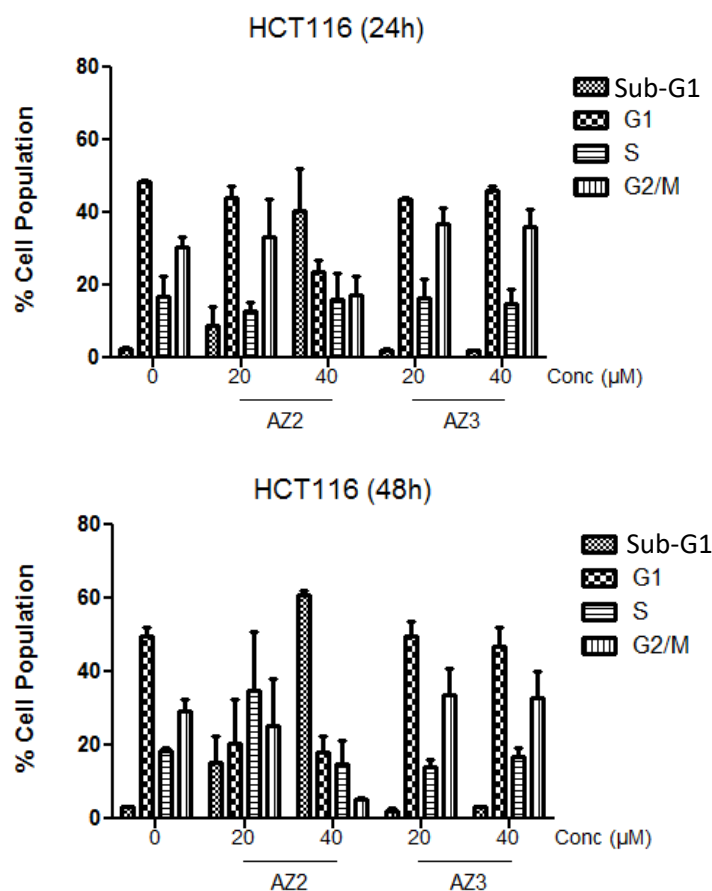
Figure S4: Cell Cycle Analysis of compound treated cells: HCT116 cells were treated with compounds (as indicated), stained with PI and analysed by flow cytometry after 24 and 48 hrs (as indicated). Cell death is evidenced by the accumulation of a sub-G1 population. Data presented as mean of at least three independent experiments. The histogram representations were derived using GraphPadPrism (GraphPad Software, Inc, La Jolla, CA).

Cell Lines	Origin	EC$_{50}$ (µM)		
		AZ1	AZ2	AZ3
HCT116	Colon	20.1	18.7	93.2
HT29	Colon	18	17.2	82.1
PC3	Prostate	22.5	23.3	>100
DU145	Prostate	23	26.2	>100
LNCap	Prostate	23.4	22	>100
T47D	Breast	15.9	16.4	97
U251	Glioblastoma	24.6	26.1	99.8
A2780	Ovarian	15.3	15.5	58.3
A431	Skin	25.2	28	>100
U937	Leukemia	9.8	11	50
A549	Lung	33.5	34.8	>100
HMEC-1	Micro vascular (normal)	32.5	30.8	>100
PANC1	Pancreatic carcinoma	19	21	87
SKOV3	Ovarian carcinoma	22	20	78
U87MG	Glioblastoma	16.5	16.5	73
U251	Glioblastoma	17	19	64
InMyoFib	Human intestinal myofibroblast	20	21	91
SW480	Corolectal adenocarcinoma	20	24	102
PANC1	Pancreatic carcinoma	19	21	87
FR2	Breast epithelial	32	33	119
T47D	Breast ductal carcinoma	17	15..5	104
MCF7	Breast adenocarcinoma	16	19	63.5
MDA231	Breast adenocarcinoma	21	24	80
HeLa	Cervix adenocarcinoma	19	22	66
NHFL	Norma human lung fibroblasts	21	35	111
Hs888LU	Norma human lung epithelial	25	30	77
H460	Lung carcinoma	26	24	70
HFFF2	Human fetal foreskin	30	29	117
PNT2	Prostate (normal)	14.3	15.5	67.6

Supplementary Table 1 – Anti-proliferative activity of AZ1-3 against a range of cancer cell lines and tissue-matched normal cell lines. Cells were treated with compounds (0-100µM) for 72 hr and viability assessment using the Cell-Titer-Glo assay (Promega). EC$_{50}$ values were derived using GraphPad Prism (GraphPad Software, Inc, La Jolla, CA) from at least two independent experiments.
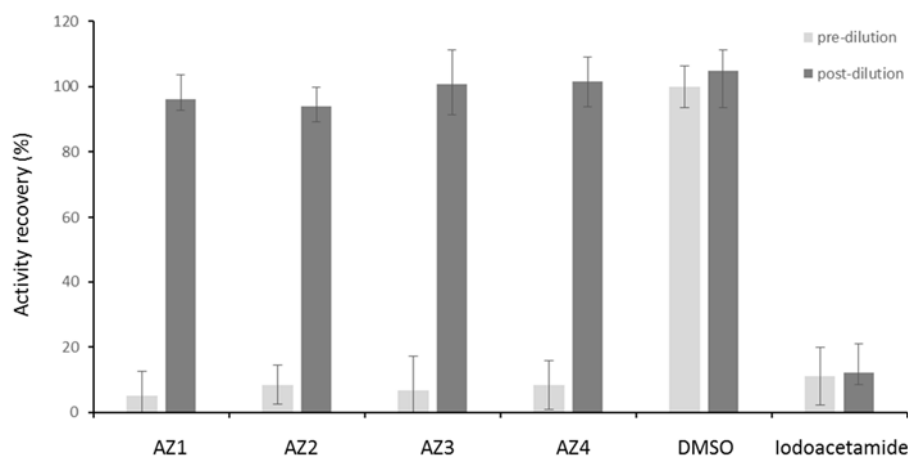
Figure S5: Reversible binding of AZ1-4 was demonstrated by high-dilution assay. USP28 was pre-incubated with 10x IC_{50} of the inhibitor or controls (based on Table 1) for 30 min followed by 100x dilution of the samples. Biochemical activity was monitored after 15 min (as described previously). Activity recovery is indicative of reversible binding following inhibitor re-equilibration. Iodoacetamide was included as a positive assay control acting as a non-specific covalent, irreversible inhibitor (cysteine alkylator). DMSO: no compound control using the same DMSO final concentration for AZ1-4. Data reported as the mean of at least 3 independent experiments with standard deviations.
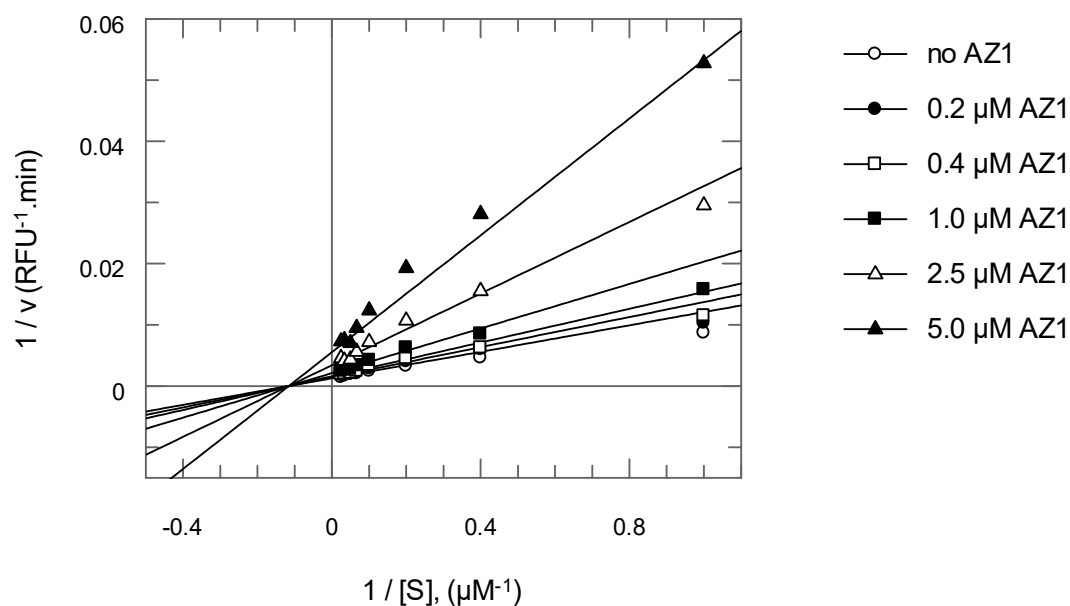
a
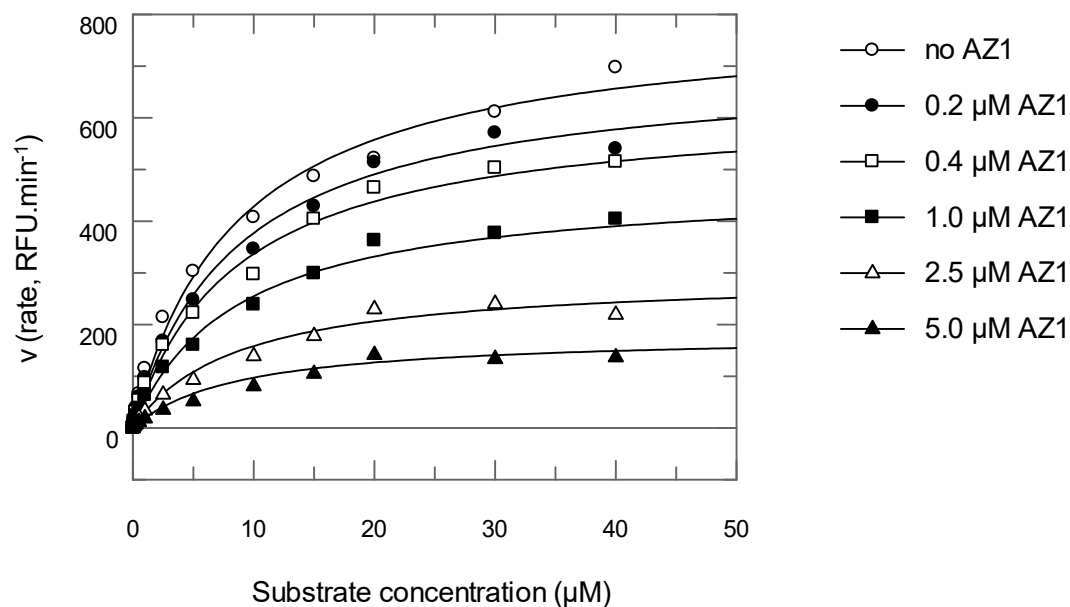
b

Figure S6: Characterisation of the mode of inhibition of USP28 by AZ1. a, Representative Michaelis-Menten plot. Inhibition was performed as indicated using varying concentrations of Tetra-Ub (from 0 to 40 µM) and inhibitor concentration (from 0 to 5.0 µM, as indicated). R-square values for fitting were >0.95 in all cases. b, Lineweaver-Burk plot (plotted using data from *A*).
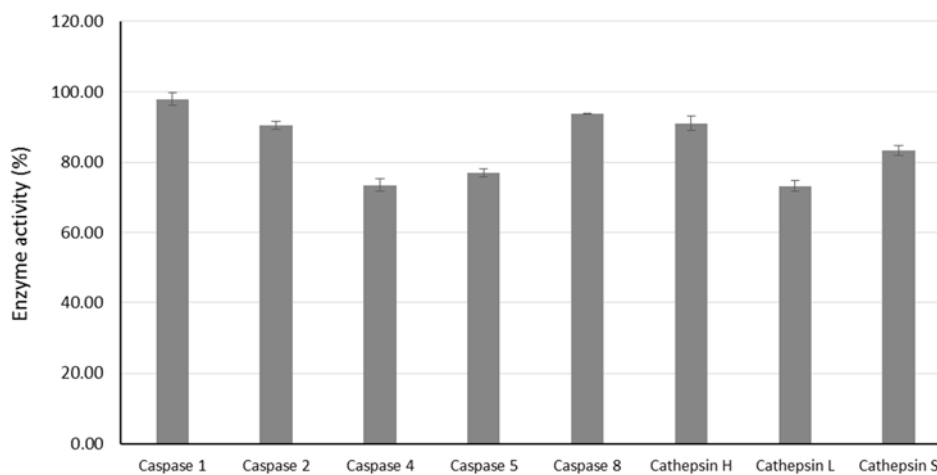
Figure S7: Selectivity profile against a panel of cysteine proteases. Representative selectivity profile of AZ1 against a panel of representative caspases and cathepsins (as indicated). AZ1 was screened at a fixed concentration of 30 µM. Data was normalised to DMSO control and reported as the mean of 2 independent experiments with standard deviations.